

**PROMINENT CONTRIBUTION OF HYDROGEN PEROXIDE TO  
INTRACELLULAR REACTIVE OXYGEN SPECIES GENERATED UPON  
EXPOSURE TO NAPHTHALENE SECONDARY ORGANIC AEROSOLS**

A Dissertation  
Presented to  
The Academic Faculty

by

Gabriela Saavedra

In Partial Fulfillment  
of the Requirements for the Degree  
Master in the  
School of Earth and Atmospheric Sciences

Georgia Institute of Technology  
August 2019

**COPYRIGHT © 2019 BY GABRIELA SAAVEDRA**

**PROMINENT CONTRIBUTION OF HYDROGEN PEROXIDE TO  
INTRACELLULAR REACTIVE OXYGEN SPECIES GENERATED UPON  
EXPOSURE TO NAPHTHALENE SECONDARY ORGANIC AEROSOLS**

Approved by:

Dr. Nga. L. Ng, Advisor  
School of Earth and Atmospheric Sciences  
*Georgia Institute of Technology*

Dr. Rodney J. Weber  
School of Earth and Atmospheric Sciences  
*Georgia Institute of Technology*

Dr. Julie A. Champion  
School of Chemical and Biomolecular Engineering  
*Georgia Institute of Technology*

Date Approved: July 24, 2019

*To my family*

## **ACKNOWLEDGEMENTS**

I would like to express my sincere gratitude to my thesis advisor, Dr Sally Ng, for the opportunity to work on this project. I deeply appreciate her enthusiasm for science and her excitement in regard to teaching. I would also like to thank my committee members, Dr. Rodney Weber and Dr. Julie Champion, for their guidance.

I would like to express the deepest appreciation to Fobang Liu for his support and patience. Without his guidance this work would not have been possible.

I would like to specially thank my family for their unfailing support and encouragement. I would like thank God for giving me the opportunity to be here.

Finally, I would like to thank my research group for their support.

## TABLE OF CONTENTS

<b>ACKNOWLEDGEMENTS</b>	<b>iv</b>
<b>LIST OF TABLES</b>	<b>vi</b>
<b>LIST OF FIGURES</b>	<b>vii</b>
<b>LIST OF SYMBOLS AND ABBREVIATIONS</b>	<b>ix</b>
<b>SUMMARY</b>	<b>xii</b>
<b>CHAPTER 1. INTRODUCTION</b>	<b>1</b>
1.1 Particulate matter and its effects on human health	1
1.2 Significance of ROS/RNS in biological systems	1
1.3 Use of H <sub>2</sub> DCF-DA to quantify intracellular ROS/RNS	3
1.4 PM components that induce the intracellular generation of ROS/RNS	4
1.5 Objective of this study	5
<b>CHAPTER 2. METHODS</b>	<b>6</b>
2.1 Laboratory Generated Naphthalene Aerosols	6
2.2 Filter Collection and Extraction	7
2.3 Determination of Intracellular ROS/RNS	8
2.4 Catalase assay	9
2.5 Amplex Red Assay	10
2.5.1 Quantification of H <sub>2</sub> O <sub>2</sub> in naphthalene SOA samples	10
2.5.2 Quantification of H <sub>2</sub> O <sub>2</sub> produced by cells	11
2.6 Statistical Analysis	12
<b>CHAPTER 3. RESULTS AND DISCUSSION</b>	<b>13</b>
3.1 Design and Optimization of Catalase assay	13
3.2 Role of H <sub>2</sub> O <sub>2</sub> in the oxidation of the probe compound	15
3.2.1 Effect of catalase on the intracellular ROS/RNS response	15
3.2.2 Investigating the oxidation of the probe compound by other ROS/RNS	17
3.3 Sources of H <sub>2</sub> O <sub>2</sub> that contributed to the oxidation of the probe compound	20
3.3.1 H <sub>2</sub> O <sub>2</sub> in naphthalene SOA samples	20
3.3.2 H <sub>2</sub> O <sub>2</sub> produced by cells	24
3.3.3 H <sub>2</sub> O <sub>2</sub> from naphthalene SOA samples and from cells were responsible for the carboxy-DCF fluorescence	26
<b>CHAPTER 4. CONCLUSIONS, IMPLICATIONS AND FUTURE WORK</b>	<b>28</b>
<b>APPENDIX A.</b>	<b>30</b>
<b>REFERENCES</b>	<b>34</b>

## LIST OF TABLES

Table A- 1	Experimental conditions and elemental composition of naphthalene SOA	30
------------	--	----

## LIST OF FIGURES

- Figure 2-A Optimized protocol for catalase assay. Cells were plated and exposed to naphthalene SOA samples containing 50 U mL<sup>-1</sup> catalase following the methodology described in Tuet et al.<sup>74</sup> Fluorescence intensity was measured after 24 h exposure with a microplate reader. Figure was modified from Tuet et al.<sup>74</sup> 10
- Figure 3-A ROS/RNS response of cells exposed to positive controls (1 µg mL<sup>-1</sup> LPS, 200 µM H<sub>2</sub>O<sub>2</sub>) without (grey) and with (orange) the addition of catalase (50 and 200 U mL<sup>-1</sup>). ROS/RNS was calculated using the fluorescent dye carboxy-H<sub>2</sub>DCFDA. Values represent the fold of change over control cells. Data are presented as mean ± SE of measurements carried out in triplicate. Statistically significant differences were determined with the *t*-test using a 90% confidence interval. \**p* = 0.08 and \**p* = 0.08, for LPS + cat 50 U mL<sup>-1</sup> and LPS + cat 200 U mL<sup>-1</sup>, respectively. \**p* = 0.05 and \**p* = 0.06 for H<sub>2</sub>O<sub>2</sub> + cat 50 U mL<sup>-1</sup> and H<sub>2</sub>O<sub>2</sub> + cat 200 U mL<sup>-1</sup>, respectively. 14
- Figure 3-B Intracellular ROS/RNS (measured as area under the dose-response curve, AUC<sup>74</sup>) induced by exposure to naphthalene SOA samples (a-d). Cells were exposed to naphthalene SOA samples only (red) and naphthalene SOA samples + 50 U mL<sup>-1</sup> catalase (blue) for 24 h. ROS/RNS measurements were carried out in triplicate, generating 3 sets of response for each naphthalene SOA sample. Each set represents the response of cells to 10 dilutions of naphthalene SOA samples (Figure A-2) and was fitted with a dose-response curve as described in Tuet et al.<sup>74</sup>. Data in this figure represent mean ± SE estimated from 3 fitted dose-response curves for each measurement. Statistically significant differences were determined with the *t*-test using a 95% confidence interval (\*\**p* = 0.001, \**p* = 0.01, \**p* = 0.03 and \**p* = 0.04 for samples a, b, c and d, respectively). 16
- Figure 3-C ROS/RNS response by cells exposed to 50, 100, 200 and 400 µM tBOOH without (red) and with (blue) catalase. 200 µM H<sub>2</sub>O<sub>2</sub> was used as a positive control. Values represent the fold increase in fluorescence over control cells. Data are presented as mean ± SE of measurements carried out in triplicate. Statistically significant differences were calculated with the *t*-test and corresponded to *p* = 0.38, *p* = 0.11, *p* = 0.38 and *p* = 0.92 for 50, 100, 200 and 400 µM tBOOH, respectively. \*\* indicates *p* < 0.01 for 200 µM H<sub>2</sub>O<sub>2</sub>. 19
- Figure 3-D H<sub>2</sub>O<sub>2</sub> produced by cells after exposure to naphthalene SOA samples (a, b, c, d) or supplemented media (control) for 24 h. The amount of H<sub>2</sub>O<sub>2</sub> produced was quantified using Amplex red. Data are presented 25

as mean  $\pm$  SE of measurements carried out in triplicate. Statistically significant differences calculated with the *t*-test corresponded to  $*p = 0.01$ ,  $*p = 0.01$ ,  $*p = 0.01$  and  $*p = 0.02$  for samples a, b, c and d compared to control, respectively.

- Figure 3-E Sources of H<sub>2</sub>O<sub>2</sub> responsible for carboxy-H<sub>2</sub>DCF fluorescence. H<sub>2</sub>O<sub>2</sub>[SOA] (blue) corresponded to the quantified H<sub>2</sub>O<sub>2</sub> using Amplex red in the absence of cells. H<sub>2</sub>O<sub>2</sub>[cell] (orange) was estimated by multiplying the rate of H<sub>2</sub>O<sub>2</sub> produced after 24 h exposure to naphthalene SOA samples (measured with Amplex red as well) by the entire exposure period (i.e., 24 h). Values represent mean  $\pm$  SE of measurements carried out in triplicate. 27
- Figure A- 1 Calibration curve for H<sub>2</sub>O<sub>2</sub> (in PBS) for the quantification of H<sub>2</sub>O<sub>2</sub> in naphthalene SOA samples (A) and released by cells (B) using Amplex red. Reactions containing Amplex red reagent, Horseradish peroxidase (HRP) and indicated amount of H<sub>2</sub>O<sub>2</sub> were incubated for 10 to 30 minutes before measuring fluorescence intensity. Values were corrected for background by subtracting the fluorescence signal from the control sample (0  $\mu$ M H<sub>2</sub>O<sub>2</sub>). 31
- Figure A-2 Dose-response curve of ROS/RNS produced by exposure to naphthalene SOA (samples a-d). Cells were exposed to naphthalene SOA extracts (A) and naphthalene SOA extracts + 50 U mL<sup>-1</sup> catalase (B) for 24 h. ROS/RNS was calculated using carboxy-H<sub>2</sub>DCFDA. Values represent the fold of change over control cells. Data are presented as means  $\pm$  SE of experiments carried out in triplicate. Every 10-dilution data was fitted with a dose-response curve as described in<sup>74</sup>. AUC data represent means  $\pm$  SE estimated from 3 dose-response fitted curves on each experiment. 32
- Figure A- 3 Quantification of H<sub>2</sub>O<sub>2</sub> produced from cells. The cells were first exposed to naphthalene SOA for 24 h. Afterwards, the fluorescence signal was measured every 15 minutes over 100 min using Amplex red. Cells were exposed to naphthalene SOA samples (orange) or supplemented media (grey) for 24 h. Values are presented as mean  $\pm$  SE of experiments carried out in triplicate. H<sub>2</sub>O<sub>2</sub> concentrations were calculated based on the calibration curves shown in Figure A-1. 33



## LIST OF SYMBOLS AND ABBREVIATIONS

A549	Human alveolar epithelial cells
AQP	Aquaporin
AUC	Area under the dose-response curve
BME	$\beta$ -mercaptoethanol
CAPS	Cavity attenuated phase shift
carboxy-DCF	carboxy-2',7'-dichlorofluorescein
carboxy-H <sub>2</sub> DCFDA	carboxy-2',7'-dichlorodihydrofluorescein diacetate
cat	Catalase
DCF	2',7'-dichlorofluorescein
FBS	Fetal bovine serum
GC-FID	Gas chromatograph flame ionization detector
GTEC	Georgia Tech Environmental Chamber
H:C	Hydrogen to carbon ratio
H <sub>2</sub> DCFDA	2',7'-dichlorodihydrofluorescein diacetate
H <sub>2</sub> O <sub>2</sub>	Hydrogen peroxide
H <sub>2</sub> O <sub>2</sub> [cells]	Amount of hydrogen peroxide produced by cells for total time of exposure
H <sub>2</sub> O <sub>2</sub> [SOA]	Amount of Hydrogen peroxide in naphthalene SOA extracted in PBS
HO <sub>2</sub>	Hydroperoxyl radical
HONO	Nitrous acid
HPAEC	Human pulmonary artery endothelial cells
HR-ToF-AMS	High resolution time-of-flight aerosol mass spectrometer
HRP	Horseradish peroxidase enzyme

IL-1 $\beta$	Interleukin 1 beta
IL-6	Interleukin 6
LPS	Lipopolysaccharide
N:C	Nitrogen to carbon ratio
MPAK	Mitogen-activated protein kinase
NAD(P)H	Nicotinamide adenine dinucleotide phosphate
NO <sub>2</sub>	Nitrogen dioxide
·NO <sub>2</sub>	Nitrogen dioxide radical
NF- $\kappa$ B	Nuclear factor kappa-light-chain-enhancer of activated B cells
NO·	Nitric Oxide
NO <sub>x</sub>	Nitrogen oxides
O:C	Oxygen to carbon ratio
O <sub>3</sub>	Ozone
O <sub>2</sub>	Oxygen
O <sub>2</sub> <sup>·-</sup>	Superoxide radical
·OH	Hydroxyl radical
ONOO <sup>-</sup>	Peroxynitrite
OS <sub>C</sub>	Average carbon oxidation state
PBS	Phosphate buffered saline
PM	Particulate matter
RH	Relative humidity
RNS	Reactive nitrogen species
RO <sub>2</sub>	Peroxyl radical
ROOH	Hydroperoxide compounds

ROS	Reactive oxygen species
ROS/RNS	Reactive oxygen and nitrogen species
SMPS	Scanning mobility particle sizer
SOA	Secondary organic aerosol
SOD	Superoxide dismutase
<i>t</i> BOOH	Tert-butyl-hydroperoxide
TNF- $\alpha$	Tumor necrosis factor- $\alpha$

## SUMMARY\*

Multiple studies have found an association between exposure to particulate matter (PM) and adverse health endpoints. One of the suggested mechanisms in which inhalable particles exert damage is by inducing the overproduction of reactive oxygen and nitrogen species (ROS/RNS). Hydrogen peroxide ( $H_2O_2$ ) is one type of ROS that has been implicated in pathological disorders induced by PM exposure. It has also received increasing attention owing to its dominant role in cellular signaling, metabolic processes, and oxidative stress. However, its biological role upon exposure to PM remains unclear. Secondary organic aerosols (SOA) make up a substantial fraction of ambient fine PM and play a role in the proinflammatory effects of the particles. In this study, the contribution of  $H_2O_2$  to intracellular ROS/RNS production upon exposure to water-soluble components of SOA generated from the photooxidation of naphthalene in the presence of  $NO_x$  (naphthalene SOA samples) was investigated using a general oxidative stress indicator (carboxy- $H_2DCFDA$ ) and a  $H_2O_2$  scavenger (catalase).

The intracellular ROS/RNS response with and without the addition of catalase to naphthalene SOA samples were measured, where the presence of catalase substantially suppressed ROS/RNS response. The  $H_2O_2$  produced by water-soluble components in the

---

\* This thesis is reproduced in part with permission from “Prominent Contribution of Hydrogen Peroxide to Intracellular Reactive Oxygen Species Generated upon Exposure to Naphthalene Secondary Organic Aerosols” by Fobang Liu, Maria G. Saavedra, Julie A. Champion, Kathy K. Griendling, and Nga L. Ng, *Environmental Science & Technology Letters*, **2020**, 7 (3), 171-177. DOI: 10.1021/acs.estlett.9b00773. Copyright © 2020 American Chemical Society.

naphthalene SOA extracted in phosphate buffer solution (PBS) was quantified and ranged from  $9.29 \pm 0.37$  to  $12.31 \pm 0.31$   $\mu\text{M}$  ( $\text{H}_2\text{O}_2[\text{SOA}]$ ), corresponding to a  $\text{H}_2\text{O}_2$  yield of 3.16 to 4.20  $\text{ng}/\mu\text{g}$ . The measured  $\text{H}_2\text{O}_2$  was product of interactions between quinone compounds and peroxide compounds in naphthalene SOA and PBS. Additionally, cells exposed to naphthalene SOA samples produced  $\text{H}_2\text{O}_2$  at a rate of  $0.21 \pm 0.01$  to  $0.26 \pm 0.03$   $\text{pmol}/\text{min}/10^4$  cells ( $\text{H}_2\text{O}_2[\text{cells}]$ ), which was associated with the mediation of immune responses and/or oxidative stress induced by naphthalene SOA exposure. These findings confirmed that  $\text{H}_2\text{O}_2$  was the main ROS produced by cells exposed to naphthalene SOA and that it was the driver of naphthalene SOA-induced ROS/RNS response, although this contribution can vary depending on the specific SOA precursors and formation conditions.

Findings in this study also showed that  $\text{H}_2\text{O}_2[\text{SOA}]$  can rapidly diffuse into the cells and contribute to the intracellular oxidation of carboxy- $\text{H}_2\text{DCF}$  to a greater extent than  $\text{H}_2\text{O}_2[\text{cells}]$ . This suggest that the diffusion of  $\text{H}_2\text{O}_2[\text{SOA}]$  into the cells represent one of the pathways in which exposure to naphthalene SOA leads to oxidative stress.

# CHAPTER 1. INTRODUCTION

## 1.1 Particulate matter and its effects on human health

Exposure to particulate matter (PM) has been recognized as a dominant cause of multiple adverse health outcomes, including cardiovascular,<sup>1-3</sup> respiratory,<sup>4-6</sup> and neurological<sup>7-9</sup> diseases, among others.<sup>10</sup> In the past decade, multiple epidemiological studies<sup>11-14</sup> have found an association between PM exposure and human measures of mortality and morbidity, while toxicological studies<sup>15-19</sup> have demonstrated its deleterious effects on tissue injuries and health endpoints. Despite these efforts, the specific mechanisms in which particles exert damage are not yet well-understood.

Multiple studies<sup>15,20-24</sup> have attributed PM adverse health endpoints to the oxidant generating properties of the particles. These particles can induce the overproduction of reactive oxygen and nitrogen species (ROS/RNS) directly by the presence of redox-active PM components in biological systems<sup>20,23,25</sup> or indirectly through interactions between particles and host proteins.<sup>26,27</sup> This overproduction of ROS/RNS can drive the uncontrolled oxidation of cellular constituents, affecting cell functionality and in some cases, causing cell death.<sup>24,28,29</sup> However, ROS/RNS have a dual role in biological systems. Other than toxic metabolites, they are necessary for the activation of multiple regulatory and metabolic processes.<sup>30-32</sup>

## 1.2 Significance of ROS/RNS in biological systems

ROS/RNS are short-lived highly reactive molecules naturally formed as byproduct of numerous physiological processes.<sup>28</sup> ROS include superoxide ( $O_2^{\cdot-}$ ), hydroxyl radicals

( $\cdot\text{OH}$ ), hydrogen peroxide ( $\text{H}_2\text{O}_2$ ), among others. RNS are commonly found as nitric oxide ( $\text{NO}\cdot$ ) and peroxynitrite ( $\text{ONOO}^-$ ).<sup>33</sup> These ROS/RNS are necessary for the regulation of multiple physiological processes, including tissue repair responses, cell growth and proliferation, apoptosis, immune mechanisms, and others.<sup>30,32,34,35</sup>

Among all ROS/RNS,  $\text{H}_2\text{O}_2$  has received increasing attention owing to its dominant role in cellular signaling, metabolic processes, and oxidative stress.<sup>36-38</sup>  $\text{H}_2\text{O}_2$  is mainly produced by spontaneous or catalytic dismutation of superoxide anions ( $\text{O}_2^-$ ) generated by the mitochondrial respiratory chain,<sup>36,39</sup> or by numerous enzymes,<sup>40</sup> such as the nicotinamide adenine dinucleotide phosphate [NAD(P)H] oxidase.<sup>41,42</sup> This oxygen metabolite has been involved in the mediation of physiological and immune responses by promoting the chemical modification of multiple proteins and transcription factors across cell membranes.<sup>37,43</sup> However,  $\text{H}_2\text{O}_2$  has also been shown to facilitate cell proliferation and cell survival of cancer cells,<sup>44</sup> which could have important implications during the progression of cancer diseases.<sup>45</sup>

$\text{H}_2\text{O}_2$  can induce different cellular responses depending on its concentration.<sup>29</sup> Low levels of  $\text{H}_2\text{O}_2$  are known to activate metabolic processes<sup>37</sup> and induce antioxidants in order to protect the cell from oxidative damage,<sup>38</sup> whereas high levels of  $\text{H}_2\text{O}_2$  stimulate the expression of pro-oxidants involved in cell cycle arrest or apoptosis,<sup>38,44</sup> as well as the hyperactivation of inflammatory responses that can result in tissue damage and pathology.<sup>29,46</sup> High levels of  $\text{H}_2\text{O}_2$  in subcellular regions, such as the mitochondria, have also been associated to hypoxia, inflammation, apoptosis, autophagy, and DNA damage,<sup>36,47</sup> which could severely affect cell viability and functionality.<sup>48</sup> Additionally,  $\text{H}_2\text{O}_2$  in the presence of transition metals, such as  $\text{Fe}^{2+}$  and  $\text{Cu}^{2+}$ , can form damaging

concentrations of hydroxyl radical ( $\text{OH}\cdot$ ).<sup>49</sup>  $\text{OH}\cdot$  is highly reactive towards lipids, proteins and DNA, and can ultimately lead to oxidative stress.<sup>44</sup>

$\text{H}_2\text{O}_2$  has also been implicated in pathological disorders induced by PM exposure, including the activation of the mitogen-activated protein kinase (MAPK) and pulmonary vasoconstriction in human pulmonary artery endothelial cells (HPAEC)<sup>50</sup> and the mediation of DNA damage in human alveolar epithelial cells (A549) by forming  $\text{OH}\cdot$  in the presence of PM water-soluble metals,<sup>51</sup> among others.<sup>17,52</sup>  $\text{H}_2\text{O}_2$  directly transported by the particles was also shown to enhance inflammatory responses and ROS formation in rats exposed to  $\text{H}_2\text{O}_2$ -fine particle mixture, resulting in tissue injury and altered alveolar macrophage activity.<sup>53</sup> These diverse pathological and physiological functions of  $\text{H}_2\text{O}_2$  have motivated multiple efforts in the development of sensitive and selective fluorescent probes to study its complex behavior in living organisms.<sup>54-58</sup> However, its biological role upon exposure to PM remains unclear.

### **1.3 Use of $\text{H}_2\text{DCF-DA}$ to quantify intracellular ROS/RNS**

PM toxicity has been widely studied using the fluorescent dye 2',7'-dichlorodihydrofluorescein diacetate ( $\text{H}_2\text{DCF-DA}$ ).<sup>17,59-62</sup> This probe was first synthesized to measure  $\text{H}_2\text{O}_2$  in cell-free systems<sup>63,64</sup> and some studies<sup>65-67</sup> used it as a marker for intracellular  $\text{H}_2\text{O}_2$  in cells exposed to PM.<sup>65-68</sup> However, it was shown that the probe compound can be oxidized by other types of ROS and RNS, such as hydroxyl radical ( $\cdot\text{OH}$ ), nitrogen dioxide ( $\cdot\text{NO}_2$ ), and peroxynitrite ( $\text{ONOO}\cdot$ ).<sup>69,70</sup> Therefore, this probe is preferably used as a qualitative index of the overall oxidative status of cells<sup>64,71,72</sup> and has been used to investigate PM-induced oxidative stress accordingly.<sup>59,60,73,74</sup> Nevertheless,



the collective use of effective  $\text{H}_2\text{O}_2$  scavengers with this probe can elucidate the role of  $\text{H}_2\text{O}_2$  in the oxidation of the probe compound,<sup>70</sup> and therefore, its contribution to PM-induced oxidative stress.

#### **1.4 PM components that induce the intracellular generation of ROS/RNS**

Ambient inhalable particles can transport redox-active compounds into biological systems that trigger the generation of ROS/RNS. Multiple studies<sup>23,25,51,75</sup> have attributed PM toxicity to the presence of water-soluble metals in the particles, which catalyze oxidants formation through Fenton-like reactions.<sup>76</sup> However, other studies<sup>20,22,77-80</sup> have found that the major fraction of the PM,<sup>81-85</sup> known as organic aerosols (OA), play an important role in the proinflammatory effects of the particles.

OA is normally dominated by secondary organic aerosols (SOA), formed from the oxidation of gas-phase compounds followed by gas-particle partitioning.<sup>81-84,86</sup> Previous studies found that SOA generated from the oxidation of the anthropogenic precursor, naphthalene, presented higher oxidative potential<sup>87,88</sup> and induced greater intracellular ROS/RNS response, as measured with  $\text{H}_2\text{DCF-DA}$ ,<sup>79</sup> than SOA from other common biogenic precursors. These effects were attributed to the presence of quinone compounds in naphthalene SOA, which offer redox active sites that serve as electron transfer intermediates.<sup>77</sup> However, the lack of specificity between the types of ROS/RNS that drove this intracellular response represents a challenge in the understanding of how naphthalene SOA exerted damage.

## 1.5 Objective of this study

In this study, the contribution of  $\text{H}_2\text{O}_2$  to the intracellular ROS/RNS response induced by water-soluble components of naphthalene SOA formed in the presence of  $\text{NO}_x$  was measured using carboxy- $\text{H}_2\text{DCFDA}$  and catalase as an effective  $\text{H}_2\text{O}_2$  scavenger. Naphthalene was chosen as the SOA precursor due to its high oxidative potential and significant impact on cellular responses, as well as a representative of polycyclic aromatic hydrocarbon (PAH) compounds that have been found in ambient fine PM.<sup>89,90</sup>  $\text{HONO}$  was used as the  $\text{OH}^\cdot$  precursor to oxidize naphthalene in order to prevent the addition of  $\text{H}_2\text{O}_2$  or  $\text{ROOH}$  compounds into the particles. The amount of  $\text{H}_2\text{O}_2$  in naphthalene SOA samples extracted in phosphate buffer solution (PBS) and produced by cells after exposure to naphthalene SOA were quantified using Amplex red, respectively. Finally, the total  $\text{H}_2\text{O}_2$  generated by cells during the complete exposure period was compared to the  $\text{H}_2\text{O}_2$  generated by naphthalene SOA samples to highlight that both  $\text{H}_2\text{O}_2$  sources could have contributed to the intracellular ROS/RNS response.

## CHAPTER 2. METHODS

### 2.1 Laboratory Generated Naphthalene Aerosols

Four SOA samples (a, b, c and d) were generated from the photooxidation of naphthalene in the presence of  $\text{NO}_x$  in the Georgia Tech Environmental Chamber (GTEC) facility, which consists of two  $12 \text{ m}^3$  Teflon chambers suspended inside a temperature-controlled enclosure surrounded by UV lights.<sup>91</sup> The four naphthalene photooxidation experiments were conducted at  $22 \text{ }^\circ\text{C}$  and  $<5\% \text{ RH}$ . The experimental conditions were similar to those in Tuet et al.<sup>92</sup> Briefly, ammonium sulfate ( $(\text{NH}_4)_2\text{SO}_4$ ) was used as seed aerosols. Naphthalene was introduced into the chamber by flowing pure air through a FEP tube containing solid naphthalene (99%, Sigma Aldrich) at  $5 \text{ L min}^{-1}$ . Nitrous acid (HONO) was used as the hydroxyl radical ( $\text{OH}^\cdot$ ) precursor to oxidize naphthalene. HONO was injected as described in Kautzman et al.<sup>93</sup> Briefly, a solution of HONO was prepared by mixing 15 mL of 1 wt % aqueous  $\text{NaNO}_2$  dropwise into 30 mL of 10 wt %  $\text{H}_2\text{SO}_4$  in a glass bulb. Then, a stream of pure air was passed through the bulb, mobilizing HONO into the chamber. Turning on the UV lights marked the beginning of the experiment.  $\text{O}_3$ ,  $\text{NO}_2$ , and  $\text{NO}_x$  concentrations were measured using an  $\text{O}_3$  analyzer (Teledyne T400), a cavity attenuated phase shift (CAPS)  $\text{NO}_2$  monitor (Aerodyne), and a chemiluminescence  $\text{NO}_x$  monitor (Teledyne 200EU), respectively. Naphthalene concentration was monitored using a gas chromatography-flame ionization detector (GC-FID, Agilent 7890A). Particle volume concentrations and size distributions were measured using a Scanning Mobility Particle Sizer (SMPS, TSI). Elemental ratios (O/C, H/C, and N/C) and average carbon oxidation state (OSc) of aerosols were characterized by a High Resolution Time-of-Flight

Aerosol Mass Spectrometer (HR-ToF-AMS, Aerodyne) with data analysis toolkits SQUIRREL (v. 1.57) and PIKA (v. 1.16G).<sup>94,95</sup> Experimental conditions and bulk aerosol chemical composition measured by the HR-ToF-AMS are summarized in Table A-1.

## 2.2 Filter Collection and Extraction

Laboratory-generated aerosols were collected on Teflon filters (47 mm, 0.45  $\mu\text{m}$  pore size, Pall Laboratory). Filter collection was initiated after the aerosol volume concentration reached its maximum<sup>93</sup> and lasted for approximately 1.5 h. The total aerosol mass collected was calculated by integrating the aerosol volume concentration data from the SMPS over the sampling time and multiplying by the total volume of air collected, as described in Tuet et al.<sup>79</sup> SMPS volume concentrations were converted to mass concentrations by assuming a density of 1.48  $\text{g cm}^{-3}$  based on prior experiments.<sup>93</sup> Blank filters containing seed aerosols and HONO only were also collected to account for background signals. The collected filter samples were stored in sterile petri dishes, sealed with parafilm, and stored at -20 °C. Prior to analysis, filters were extracted following established protocols<sup>74,79,87,96</sup> where the filters were submerged in RPMI-1640 media (for exposure experiments) or phosphate buffer solution (PBS) (for quantification of  $\text{H}_2\text{O}_2$  in naphthalene SOA samples only) and sonicated for 30 minutes using an Ultrasonic Cleanser (VWR International). Naphthalene SOA samples were filtered with 0.45  $\mu\text{m}$  PTFE syringe filters (Fisherbrand<sup>TM</sup>) and the ones submerged in RPMI-1640 media were supplemented with 10 % Fetal Bovine Serum (FBS).

### 2.3 Determination of Intracellular ROS/RNS

The intracellular ROS/RNS generated upon exposure to water-soluble components of naphthalene SOA (naphthalene SOA samples a, b, c, and d, respectively) extracted in RPMI-1640 medium were measured using the oxidation-sensitive fluorescent probe 5-(and-6)-carboxy-2',7'-dichlorodihydrofluorescein diacetate (carboxy-H<sub>2</sub>DCFDA, Molecular Probes C-400). This compound becomes deacetylated by intracellular esterases and is better retained intracellularly due to its additional negative charges.<sup>97</sup> The non-fluorescent deacetylated compound is oxidized by the activity of ROS/RNS species, forming the fluorescent compound carboxy-DCF.

The protocol followed was the one established in our previous studies.<sup>74,79,92</sup> Briefly, a 96 well-plate was pre-coated with 10 % Fetal Bovine Serum (FBS) dissolved in PBS. Immortalized murine alveolar macrophages MH-S (ATCC® CRL-2019™) cultured in RPMI-1640 (ATCC® 30-2001™) supplemented with 10% Fetal Bovine Serum (FBS), 1% penicillin-streptomycin, and 50 μM β-mercaptoethanol (BME) were seeded onto the pre-coated plate at a density of  $2 \times 10^4$  cells well<sup>-1</sup> and incubated overnight. Then, cells were stained with carboxy-H<sub>2</sub>DCFDA by replacing the cell medium with the probe solution at a concentration of 10 μM. After incubation for 40 minutes with the probe solution, cells were exposed to naphthalene SOA and control samples in triplicate for 24 h. The naphthalene SOA samples consisted on a set of 10 dilutions of naphthalene SOA extract in supplemented media to capture the specific dose-response region for each sample.<sup>74</sup> The positive controls included H<sub>2</sub>O<sub>2</sub> (200 μM) and Lipopolysaccharide (LPS, 1 μg mL<sup>-1</sup>), and the negative control corresponded to non-stained cells exposed to only media (no

stimulants). After 24 h exposure, the medium was replaced with PBS and placed in a microplate reader (BioTek Synergy H4) to measure fluorescence intensity at 485 nm excitation and 525 nm emission.

## **2.4 Catalase assay**

The catalase assay protocol was based on previous studies where catalase was used as an effective H<sub>2</sub>O<sub>2</sub> scavenger<sup>98,99</sup> but optimized in this study to ensure its functionality when using an adherent macrophage cell line (ATCC® CRL-2019™). The optimized protocol is shown in Figure 2-A. Briefly, cells were plated and exposed to the probe (carboxy-H<sub>2</sub>DCFDA, Molecular Probes C-400) following steps (1) to (3) of our intracellular ROS/RNS protocol.<sup>74</sup> Step (4) involved replacing the ROS/RNS probe solution with four naphthalene SOA samples (a, b, c and d, respectively) containing 50 U mL<sup>-1</sup> catalase. H<sub>2</sub>O<sub>2</sub> (200 μM) was used as a positive control and not stained cells exposed to probe solution only corresponded to the negative control. Stained cells exposed to only supplemented media or catalase (50 U mL<sup>-1</sup>) were used to correct the background ROS/RNS signal. After 24 h of incubation, the medium was removed and replaced with phosphate buffer solution (PBS). Lastly, the plate was placed in a microplate reader (BioTek Synergy H4) to measure the fluorescence intensity at excitation of 485 nm and emission of 528 nm (5).

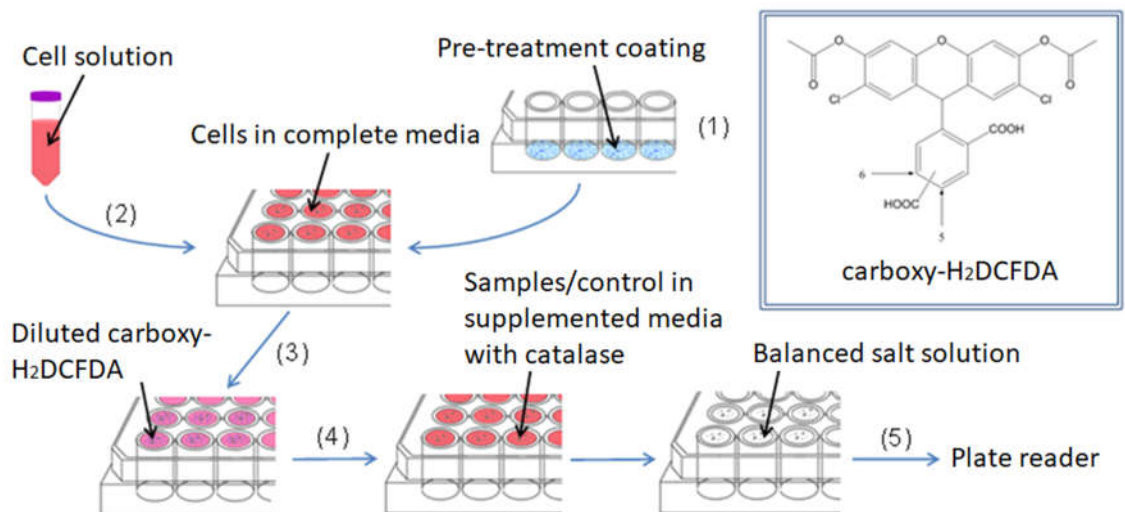


**Figure 2-A. Optimized protocol for catalase assay.** Cells were plated and exposed to naphthalene SOA samples containing  $50 \text{ U mL}^{-1}$  catalase following the methodology described in Tuet et al.<sup>74</sup> Fluorescence intensity was measured after 24 h exposure with a microplate reader. Figure was modified from Tuet et al.<sup>74</sup>

## 2.5 Amplex Red Assay

Amplex red assay has been widely used to detect H<sub>2</sub>O<sub>2</sub> activity in biological samples and enzymatic processes.<sup>100</sup> In the presence of the enzyme horseradish peroxidase (HRP), the highly sensitive Amplex red reagent (10-acetyl-3, 7-dihydroxyphenoxazine) is oxidized by H<sub>2</sub>O<sub>2</sub>, forming a red-fluorescent compound.<sup>101</sup> In this study, Amplex™ Red Hydrogen Peroxide kit (A22188, Molecular Probes) was used to determine the content of H<sub>2</sub>O<sub>2</sub> present in naphthalene SOA samples and produced by cells after 24 h exposure to naphthalene SOA samples.

### 2.5.1 Quantification of H<sub>2</sub>O<sub>2</sub> in naphthalene SOA samples

The H<sub>2</sub>O<sub>2</sub> concentration in the water-soluble fraction of naphthalene SOA extracted in PBS was quantified using Amplex red. Firstly, 50  $\mu\text{L}$  of naphthalene SOA extracted in PBS

were placed in a 96 well-plate. Then, 50  $\mu\text{L}$  of working solution (100  $\mu\text{M}$  Amplex red reagent and 0.2  $\text{U mL}^{-1}$  HRP diluted in 1X Reaction Buffer) were added to each extract. Fluorescence intensity was measured after 30 min incubation at an excitation of 530 nm and emission of 590. Measurements were corrected from background by subtracting the fluorescence signal from the control sample (0  $\mu\text{M}$   $\text{H}_2\text{O}_2$ ).  $\text{H}_2\text{O}_2$  concentrations were calculated based on a calibration curve of  $\text{H}_2\text{O}_2$  concentrations ranging from 0 to 10  $\mu\text{M}$  in PBS (Figure A-1).  $\text{H}_2\text{O}_2$  standard curve concentrations were based on the amounts of  $\text{H}_2\text{O}_2$  quantified on extracts from ambient PM and SOA from different organic precursors.<sup>102</sup> Additionally,  $\text{H}_2\text{O}_2$  was quantified in naphthalene SOA samples with the addition of 50  $\text{U mL}^{-1}$  catalase.

### 2.5.2 *Quantification of $\text{H}_2\text{O}_2$ produced by cells*

Amplex red reagent remains outside the cell, reacting with  $\text{H}_2\text{O}_2$  that diffuses from the cell into the medium. Therefore, it is a measure of extracellular  $\text{H}_2\text{O}_2$ . Briefly, cells were plated and exposed to naphthalene SOA samples for 24 h following the intracellular ROS/RNS assay (without the addition of carboxy- $\text{H}_2\text{DCFDA}$ ). After exposure time, cell medium was replaced by 100  $\mu\text{L}$  of working solution (PBS containing 50  $\mu\text{L}$  of Amplex red and 0.1  $\text{U mL}^{-1}$  HRP). The plate was incubated at 37  $^\circ\text{C}$  and 5%  $\text{CO}_2$  for 10 minutes and then, it was placed in a microplate reader to measure fluorescence intensity every 15 minutes over a period of 100 minute.<sup>16</sup> Fluorescence values were corrected from background. The  $\text{H}_2\text{O}_2$  concentration was calculated based on a calibration curve of  $\text{H}_2\text{O}_2$  concentrations ranging from 0 to 1  $\mu\text{M}$  in PBS (Figure A-1).



## **2.6 Statistical Analysis**

Exposure experiments were performed once. All results are shown as mean  $\pm$  SE of independent experiments performed in triplicate. Statistical significance of the data was calculated using the un-paired, two tailed *t*-test with confidence intervals of 90% and 95%, respectively.

## CHAPTER 3. RESULTS AND DISCUSSION

### 3.1 Design and Optimization of Catalase assay

Previous studies have shown that cells treated with catalase can mitigate the effects of redox insults and effectively reduce ROS/RNS signal.<sup>98,99,103–107</sup> However, there are substantial variations in the employed methodologies depending on cell lines used, time of treatment with catalase, fluorescent dyes, and stimulants tested. In order to ensure comparability with our optimized intracellular ROS/RNS assay,<sup>74</sup> a protocol using catalase as a H<sub>2</sub>O<sub>2</sub> scavenger was designed to evaluate its role in naphthalene SOA-induced ROS/RNS response. The parameters to optimize included time duration of treating the cells with catalase and catalase concentration. In previous studies,<sup>105–107</sup> cells were pretreated with catalase for a range 0.5 to 4 h before exposing them to stimulants. However, these studies used specific features to facilitate the intracellular access of the catalase, a macromolecule, to cellular and subcellular regions.<sup>107</sup> In this study, the catalase was added to naphthalene SOA samples at a specific concentration and incubated for 24 h to ensure that there was sufficient time for the catalase to interact and/or be absorbed by the cells. The chosen time of exposure was based on the stability of catalase for 24 h at 37°C<sup>108,109</sup> and on the exposure time used in the intracellular ROS/RNS assay.<sup>74</sup>

The catalase concentration was determined by exposing macrophage cells to positive controls (1 µg mL<sup>-1</sup> LPS and 200 µM H<sub>2</sub>O<sub>2</sub>) with the addition of 0, 50, and 200 U mL<sup>-1</sup> catalase (Sigma-Aldrich, C-3515), which are concentrations that are generally used in prior studies.<sup>98,99</sup> As shown in Figure 3-A, LPS and H<sub>2</sub>O<sub>2</sub> induced a response of 1.5-fold compared to control cells. The addition of 50 and 200 U mL<sup>-1</sup> catalase fairly decrease ( $p <$

0.1) the ROS/RNS signal induced by LPS and H<sub>2</sub>O<sub>2</sub> to control values. This confirmed that catalase removed the species that mediated the oxidation of the probe compound and that the protocol can be used to identify reactive species that drive ROS/RNS response. The difference in the response after treating the cells with 50 and 200 U mL<sup>-1</sup> catalase was not significant ( $p = 0.9$ ), therefore, the chosen concentration of catalase was 50 U mL<sup>-1</sup>.

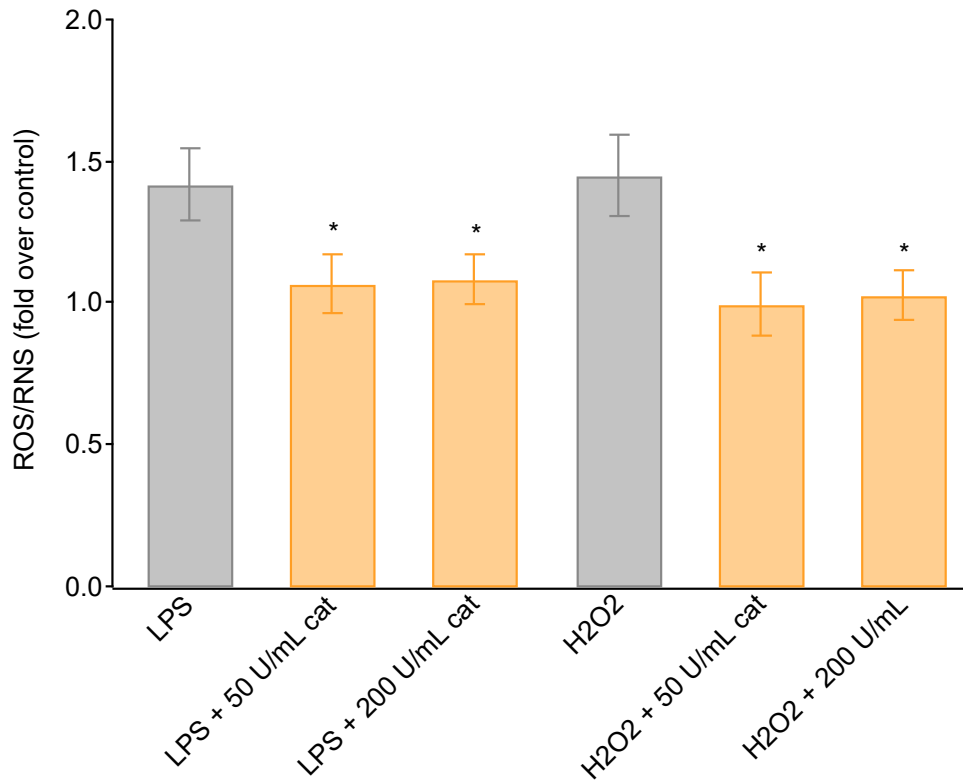


**Figure 3-A. ROS/RNS response of cells exposed to positive controls (1  $\mu\text{g mL}^{-1}$  LPS, 200  $\mu\text{M}$  H<sub>2</sub>O<sub>2</sub>) without (grey) and with (orange) the addition of catalase (50 and 200 U mL<sup>-1</sup>). ROS/RNS was calculated using the fluorescent dye carboxy-H<sub>2</sub>DCFDA. Values represent the fold of change over control cells. Data are presented as mean  $\pm$  SE of measurements carried out in triplicate. Statistically significant differences were determined with the *t*-test using a 90% confidence interval. \* $p = 0.08$  and \* $p = 0.08$ , for LPS + cat 50 U mL<sup>-1</sup> and LPS + cat 200 U mL<sup>-1</sup>, respectively. \* $p = 0.05$  and \* $p = 0.06$  for H<sub>2</sub>O<sub>2</sub> + cat 50 U mL<sup>-1</sup> and H<sub>2</sub>O<sub>2</sub> + cat 200 U mL<sup>-1</sup>, respectively.**

## 3.2 Role of H<sub>2</sub>O<sub>2</sub> in the oxidation of the probe compound

### 3.2.1 Effect of catalase on the intracellular ROS/RNS response

Intracellular ROS/RNS generation upon exposure to naphthalene SOA samples was measured using carboxy-H<sub>2</sub>DCFDA. Carboxy-H<sub>2</sub>DCF is better retained intracellularly than other probes due to its additional two charges<sup>97</sup> and is oxidized by ROS/RNS species forming the fluorescent compound carboxy-DCF.<sup>110</sup> Figure 3-B shows the ROS/RNS response with and without the addition of catalase. In samples without the addition of catalase, naphthalene SOA-induced ROS/RNS response exhibited a dose-dependent manner (Figure A-2A) similar to those reported in previous studies.<sup>79,92</sup> Prior studies have shown that there is a correlation between ROS/RNS response and the degree of oxidation (photochemical aging) of aerosol samples.<sup>92</sup> The four naphthalene SOA samples in this study had relatively lower carbon oxidation states and induced lower but still appreciable ROS/RNS response. Nevertheless, the ROS/RNS production observed in this study was comparable to the results in Tuet et al.<sup>92</sup> for naphthalene SOA with similar oxidation state. The ROS/RNS response of the samples with the addition of catalase was significantly lower ( $*p < 0.05$ ) than the ROS/RNS response without catalase (Figure 3-B). This suggests that catalase effectively removed the compounds that mediated ROS/RNS response.

Catalase is a heme-containing enzyme that catalytically breaks down H<sub>2</sub>O<sub>2</sub> into unreactive molecules of H<sub>2</sub>O and O<sub>2</sub>. It presents the highest affinity for H<sub>2</sub>O<sub>2</sub>, although it can oxidize other substrates but at significantly slower rates than the decomposition of H<sub>2</sub>O<sub>2</sub>.<sup>111,112</sup> Prior studies have reported that catalase-containing media improves cell survival and supports cell growth in different cell lines through hormone-receptor interactions or cellular

absorption of catalase, which eliminates intracellular  $\text{H}_2\text{O}_2$  toxicity.<sup>113–115</sup> Similarly, multiple studies have found a decrease in intracellular ROS/RNS response after catalase addition,<sup>116–120</sup> which is in accordance with the results in this study. These findings imply the role of  $\text{H}_2\text{O}_2$  as the mediator of ROS/RNS signal. However, the probe compound can also be oxidized by other types of ROS/RNS that could have been produced by cells upon exposure to naphthalene SOA, such as hydroxyl radical ( $\cdot\text{OH}$ ), nitrogen dioxide ( $\cdot\text{NO}_2$ ), and peroxyxynitrite ( $\text{ONOO}\cdot$ ).

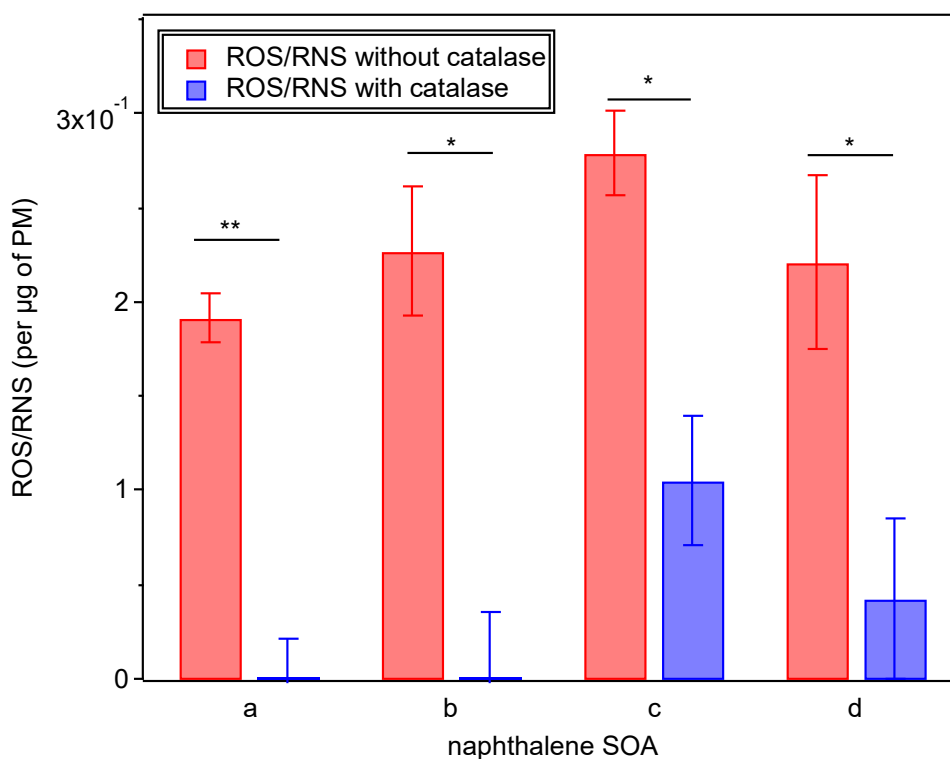
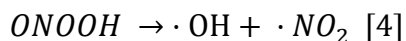
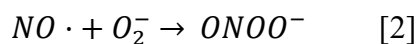
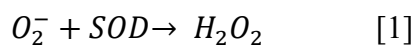


**Figure 3-B. Intracellular ROS/RNS (measured as area under the dose-response curve,  $\text{AUC}^{74}$ ) induced by exposure to naphthalene SOA samples (a-d). Cells were exposed to naphthalene SOA samples only (red) and naphthalene SOA samples +  $50 \text{ U mL}^{-1}$  catalase (blue) for 24 h. ROS/RNS measurements were carried out in triplicate, generating 3 sets of response for each naphthalene SOA sample. Each set represents the response of cells to 10 dilutions of naphthalene SOA samples (Figure A-2) and was fitted with a dose-response curve as described in Tuet et al.<sup>74</sup>. Data in this figure**

represent mean  $\pm$  SE estimated from 3 fitted dose-response curves for each measurement. Statistically significant differences were determined with the *t*-test using a 95% confidence interval (\*\**p* = 0.001, \**p* = 0.01, \**p* = 0.03 and \**p* = 0.04 for samples a, b, c and d, respectively).

### 3.2.2 Investigating the oxidation of the probe compound by other ROS/RNS

Cells normally generate ROS and RNS as part of metabolic processes or induced by exogenous factors. Superoxide ( $O_2^-$ ) can be formed under physiological processes, such as the mitochondrial respiration chain,<sup>30,121</sup> or by redox cycling reactions driven by quinone compounds.<sup>122</sup>  $O_2^-$  directly generates  $H_2O_2$  through the dismutation reaction that occurs either spontaneously or enzymatically by superoxide dismutases (SOD) [equation 1].<sup>123</sup> Nitric oxide ( $NO\cdot$ ) is also generated under physiological and pathological conditions, induced by nitric oxide synthases (iNOS). This nitrogen metabolite can react with  $O_2^-$  to form peroxynitrite ( $ONOO^-$ ) [equation 2].  $ONOO^-$  is in equilibrium with peroxynitrous acid ( $ONOOH$ ) [equation 3] and both species are important oxidizing agents *in vivo*.<sup>124</sup> However, the protonation of  $ONOO^-$  weakens the O-O bond and causes its rapid decomposition into  $\cdot OH$  and  $\cdot NO_2$  [equation 4].<sup>125</sup>



The oxidation of H<sub>2</sub>DCF by these types of ROS and RNS has been extensively discussed in literature.<sup>64,126</sup> For instance, H<sub>2</sub>DCF showed very low or no reactivity towards O<sub>2</sub><sup>-127</sup> and its reaction with H<sub>2</sub>O<sub>2</sub> is catalyzed by the intervention of biological substances.<sup>64,126,128</sup> ·NO<sub>2</sub> can efficiently convert H<sub>2</sub>DCF into DCF ( $k \sim 1.7 \times 10^7 \text{ M}^{-1}\text{s}^{-1}$ )<sup>69</sup>. Similarly, ·OH reacts with H<sub>2</sub>DCF at a faster rate ( $k \sim 1.3 \times 10^{10} \text{ M}^{-1} \text{ s}^{-1}$ ) than its reaction with catalase and H<sub>2</sub>O<sub>2</sub> (complex 1) ( $k \sim 10^7 \text{ M}^{-1} \text{ s}^{-1}$ ).<sup>69,129</sup> Therefore, both species should be able to oxidize H<sub>2</sub>DCF even in the presence of catalase. Due to the lack of response after catalase addition (Figure 3-B), it can be concluded that ·OH and ·NO<sub>2</sub> did not contribute to the oxidation of carboxy-H<sub>2</sub>DCF upon exposure to naphthalene SOA. NO· does not readily oxidize H<sub>2</sub>DCF,<sup>126</sup> but some of its derivatives can efficiently oxidize the probe, such as ONOO·.<sup>130</sup> The rate of reaction between O<sub>2</sub><sup>-</sup> and NO· ( $k \sim 10^{10} \text{ M}^{-1} \text{ s}^{-1}$ )<sup>124</sup> [equation 2] is an order of magnitude faster than the enzymatic dismutation of O<sub>2</sub><sup>-</sup> driven by SOD ( $k \sim 2 \times 10^9 \text{ M}^{-1} \text{ s}^{-1}$ )<sup>131</sup> [equation 1], but under physiological conditions SOD levels (~μM) normally exceed NO· levels (~nM), making H<sub>2</sub>O<sub>2</sub> formation [equation 1] more important.<sup>125</sup> Under pathological conditions induced by PM exposure, both NO· levels and SOD activity have been shown to increase.<sup>132-134</sup> However, the presence of H<sub>2</sub>O<sub>2</sub> in this study implies that SOD levels were higher than NO· levels and that the generation of ONOO· was negligible.

Other compounds that can oxidize H<sub>2</sub>DCF are organic peroxides (ROOH), such as tert-butyl-hydroperoxide (*t*BOOH).<sup>135,136</sup> Peroxide compounds were likely present in the naphthalene SOA samples used in this study<sup>93</sup> and can be decomposed by catalase.<sup>137</sup> In order to investigate the selectivity of catalase towards decomposition of H<sub>2</sub>O<sub>2</sub> and/or ROOH compounds, the ROS/RNS response of cells exposed to *t*BOOH was measured with and without the addition of catalase. The presence of catalase did not decrease the

ROS/RNS response induced by *t*BOOH, but significantly decreased ( $*p < 0.05$ ) the ROS/RNS response induced by H<sub>2</sub>O<sub>2</sub> to control values (Figure 3-C). This suggests that catalase specifically decomposed H<sub>2</sub>O<sub>2</sub> in our system and confirms that the removal of H<sub>2</sub>O<sub>2</sub> caused the inhibition of ROS/RNS response (Figure 3-B).

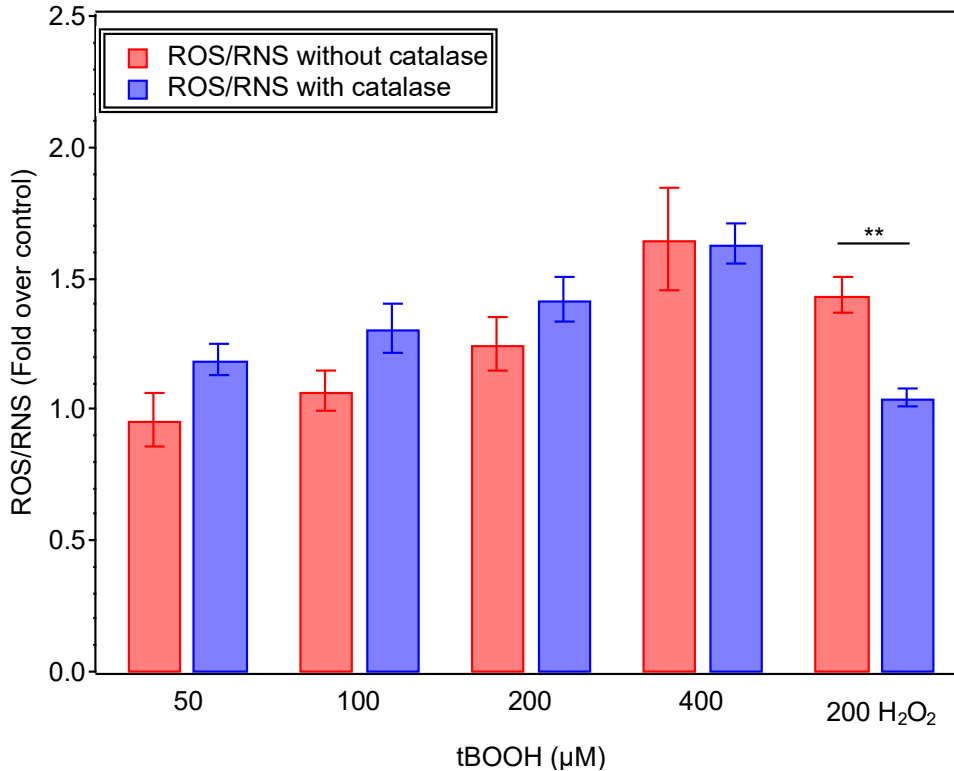


**Figure 3-C. ROS/RNS response by cells exposed to 50, 100, 200 and 400 μM *t*BOOH without (red) and with (blue) catalase. 200 μM H<sub>2</sub>O<sub>2</sub> was used as a positive control. Values represent the fold increase in fluorescence over control cells. Data are presented as mean ± SE of measurements carried out in triplicate. Statistically significant differences were calculated with the *t*-test and corresponded to  $p = 0.38$ ,  $p = 0.11$ ,  $p = 0.38$  and  $p = 0.92$  for 50, 100, 200 and 400 μM *t*BOOH, respectively. \*\* indicates  $p < 0.01$  for 200 μM H<sub>2</sub>O<sub>2</sub>.**

As shown in Figure 3-B, the ROS/RNS response expressed as area under the curve (AUC) for samples c was not totally suppressed after catalase addition. It should be noted that the ROS/RNS response expressed as fold over control for this sample (Figure A-2B) did not



follow a dose-response relationship as in Figure A-2A and that the fitted curve was influenced by the dispersion of the data from measurements performed in triplicate. Furthermore, the AUC calculated for this sample was not statistically different from the other three samples ( $p = 0.20$ ). This implies that the AUC calculated for samples c arose from experimental uncertainties and thus, is insignificant. Taken together, the significant inhibition of ROS/RNS signal after catalase addition in the four samples confirms the role of  $H_2O_2$  as the main driver of the carboxy-DCF fluorescence induced by naphthalene SOA exposure. However, previous studies<sup>102,138-140</sup> have reported the presence of  $H_2O_2$  in PM samples alone. The question remains as to whether both  $H_2O_2$  in naphthalene SOA samples and generated by cells contributed to the measured carboxy-DCF fluorescence. And if so, how much was the contribution from each source?

### **3.3 Sources of $H_2O_2$ that contributed to the oxidation of the probe compound**

#### *3.3.1 $H_2O_2$ in naphthalene SOA samples*

The  $H_2O_2$  concentration in the water-soluble fraction of naphthalene SOA extracted in PBS ( $H_2O_{2[SOA]}$ ) was quantified using Amplex red. It should be noted that the four naphthalene photooxidation experiments were performed in the presence of  $NO_x$  and under dry conditions. These conditions were selected to prevent the formation of ROOH compounds, making  $RO_2 + NO$  the dominant reaction pathway, and to avoid the addition of  $H_2O_2$  into the particles. The bulk chemical composition of the four samples, was very similar (Table A-1), as well as the quantified  $H_2O_2$ , which ranged slightly from  $9.29 \pm 0.37$  to  $12.31 \pm 0.31 \mu M$ , corresponding to a  $H_2O_2$  yield of 3.16-4.20 ng/ $\mu g$ . The presence of  $H_2O_2$  in naphthalene SOA samples was further confirmed by adding catalase to the samples, where

catalase completely decomposed the  $\text{H}_2\text{O}_2$  in all naphthalene SOA samples as expected.  $\text{H}_2\text{O}_{2[\text{SOA}]}$  could be produced by interactions between different compounds in naphthalene SOA and the extraction solution (PBS). Both quinone compounds<sup>141</sup> and organic peroxides<sup>93</sup> have been detected in naphthalene SOA and both can produce  $\text{H}_2\text{O}_2$  in aqueous-phase reactions.<sup>88,138,139,142–144</sup> However, Kautzman et al.<sup>93</sup> found that organic peroxides contributed to less than 30 % of the total SOA mass produced by the photooxidation of naphthalene in the presence of  $\text{NO}_x$ . Furthermore, Tong et al.<sup>102</sup> attributed a  $\text{H}_2\text{O}_2$  yield of  $1.99 \pm 0.33$  ng/ $\mu\text{g}$  of naphthalene SOA in water to the presence of quinone compounds and their results were comparable to the  $\text{H}_2\text{O}_2$  yield in this study (3.16-4.20 ng/ $\mu\text{g}$ ). Therefore, it is likely that the  $\text{H}_2\text{O}_{2[\text{SOA}]}$  in this study mostly originated from quinoid redox cycling driven by quinone compounds.<sup>141</sup> The generation of  $\text{H}_2\text{O}_2$  by quinone compounds has been reported in multiple solvents<sup>145</sup> and has been shown to be catalyzed by interactions between endogenous antioxidants and semiquinones in biological systems.<sup>102,146</sup> This suggest that the quantified  $\text{H}_2\text{O}_{2[\text{SOA}]}$  could be produced in biological systems, which can disturb the cellular redox balance and lead to oxidative stress.<sup>147</sup> It should be noted that  $\text{H}_2\text{O}_{2[\text{SOA}]}$  was quantified in naphthalene SOA extracted in PBS due to the fluorescence interference of RPMI-1640 media. Therefore,  $\text{H}_2\text{O}_{2[\text{SOA}]}$  could be different from the  $\text{H}_2\text{O}_2$  produced by naphthalene SOA samples (naphthalene SOA extracted in RPMI-1640 media). Future studies are suggested to investigate the impact of extraction solvents on the generation of  $\text{H}_2\text{O}_2$  in aerosol samples.<sup>148</sup>

It is known that extracellular  $\text{H}_2\text{O}_2$  can easily diffuse into cellular cytosols to promote redox signals through aquaporin (AQP) channels.<sup>149</sup> Besides facilitating  $\text{H}_2\text{O}_2$  intracellular signaling functions, these channels have also been implicated in the activation of cellular

immune responses.<sup>150–152</sup> Previous studies<sup>153,154</sup> found that AQP channels mediated the production of important proinflammatory cytokines upon stimuli, such as TNF- $\alpha$  and IL-1 $\beta$ . These cytokines have been shown to be produced by macrophages exposed to PM samples containing quinone compounds.<sup>79,155</sup> This suggests that in this study, exposure to naphthalene SOA increased AQP activity, facilitating the transport of H<sub>2</sub>O<sub>2</sub> across the cell membrane. In order to investigate the diffusion of H<sub>2</sub>O<sub>2</sub>[SOA] into cells, cells were plated and stained with the probe following steps (1) to (3) of our intracellular ROS/RNS protocol.<sup>74</sup> Step (4) involved replacing the ROS/RNS probe solution with naphthalene SOA samples extracted in PBS. H<sub>2</sub>O<sub>2</sub> in stained cells exposed to naphthalene SOA was quantified every 15 minutes over 1 h exposure. At each time point, 50  $\mu$ L of cellular medium (PBS) containing naphthalene SOA was transferred to a 96 well plate. Additionally, 50  $\mu$ L of each naphthalene SOA sample without interaction of cells was added to an empty well to evaluate the rate of decomposition of H<sub>2</sub>O<sub>2</sub>[SOA]. Then, the reaction was started by adding 50  $\mu$ L of Amplex red reagent to each well with the samples. After 30 minutes incubation at room temperature based on the Amplex red protocol (Invitrogen), fluorescence was measured.

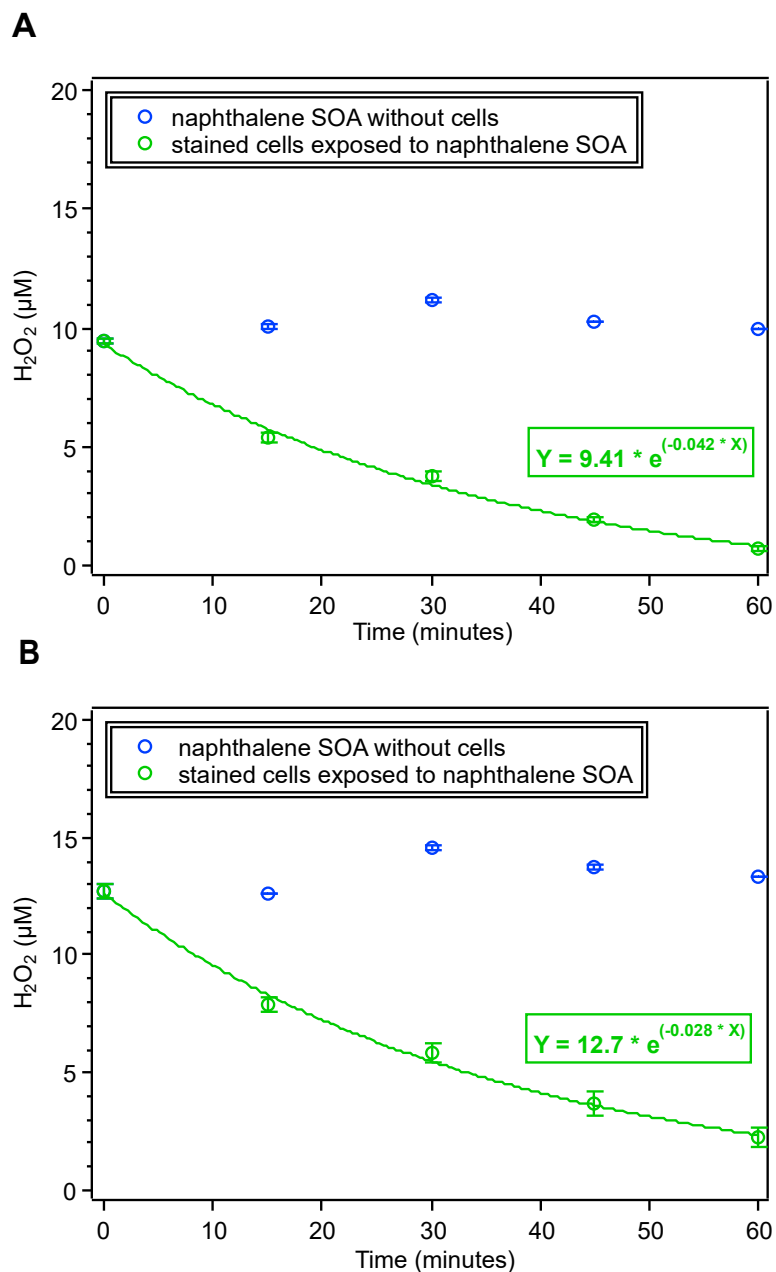


**Figure 3-D. Quantification of H<sub>2</sub>O<sub>2</sub> in stained cells exposed to naphthalene SOA samples b (A) and d (B).** “H<sub>2</sub>O<sub>2</sub> in naphthalene SOA extracts without cells” corresponds to the potential decomposition of H<sub>2</sub>O<sub>2</sub>[SOA]. “H<sub>2</sub>O<sub>2</sub> in stained cells exposed to naphthalene SOA” corresponds to the concentration of H<sub>2</sub>O<sub>2</sub> in cell medium of cells stained with the ROS probe containing naphthalene SOA. H<sub>2</sub>O<sub>2</sub> was quantified using Amplex red. Data are presented as mean ± SE of measurements carried out in triplicate.

As shown in Figure 3-D,  $\text{H}_2\text{O}_{2[\text{SOA}]}$  presented an 80% decrease in the presence of cells after 1 h, while  $\text{H}_2\text{O}_{2[\text{SOA}]}$  without cells was stable over time. Hence, it was very likely that the  $\text{H}_2\text{O}_{2[\text{SOA}]}$  diffused into the cells and contributed to the intracellular oxidation of carboxy- $\text{H}_2\text{DCF}$ . Note that the possibility of  $\text{H}_2\text{O}_2$  decomposition on the surface of the cell or by interaction with other components produced by cells is not excluded in this study.

### 3.3.2 $\text{H}_2\text{O}_2$ produced by cells

The  $\text{H}_2\text{O}_2$  produced by cells after being exposed to naphthalene SOA samples for 24 h ( $\text{H}_2\text{O}_{2[\text{cells}]}$ ) was also measured using Amplex red (Figure 3-E). It should be noted that cells were first exposed to naphthalene SOA samples for 24 h, and then, the cell medium containing naphthalene SOA samples was replaced with the Amplex red working solution. Therefore, the quantified  $\text{H}_2\text{O}_2$  corresponds to the  $\text{H}_2\text{O}_2$  produced by the cell only after interacting with naphthalene SOA samples for 24 h. Intracellularly,  $\text{H}_2\text{O}_2$  can be produced by the enzymatic oxidation of quinone compounds,<sup>122,141</sup> which were likely present in the naphthalene SOA samples, and is also generated by cells to activate the transcription factor  $\text{NF-}\kappa\text{B}$ <sup>120,156,157</sup> and its related cytokines  $\text{TNF-}\alpha$  and  $\text{IL-6}$ ,<sup>158</sup> which were both expressed by cells exposed to naphthalene SOA as shown in previous studies.<sup>159</sup> In agreement with these findings, exposure to naphthalene SOA samples induced the production rates of  $\text{H}_2\text{O}_2$  ranging from  $0.21 \pm 0.01$  to  $0.26 \pm 0.03$  pmol/min/ $10^4$  cells (Figure 3-E). The production rates were calculated from the  $\text{H}_2\text{O}_2$  concentration measured at different time points after the 24 h exposure (Figure A-3). Assuming the capacity of cells to produce  $\text{H}_2\text{O}_2$  is constant over time, the total amount of  $\text{H}_2\text{O}_2$  produced by cells exposed to naphthalene SOA was

calculated by multiplying the rate of H<sub>2</sub>O<sub>2</sub> produced by the exposure time (24 h). Results show that cells could have produced 3.02 ± 0.01 to 3.74 ± 0.03 μM H<sub>2</sub>O<sub>2</sub> over the 24 h of exposure to naphthalene SOA. This H<sub>2</sub>O<sub>2</sub> production could be associated to the mediation of adverse health outcomes and/or immune responses induced by exposure to naphthalene SOA. Future studies are warranted to investigate potential time variabilities in the capability of cells to produce H<sub>2</sub>O<sub>2</sub> upon PM exposure to study the biological significance of the exposure time used in this study.

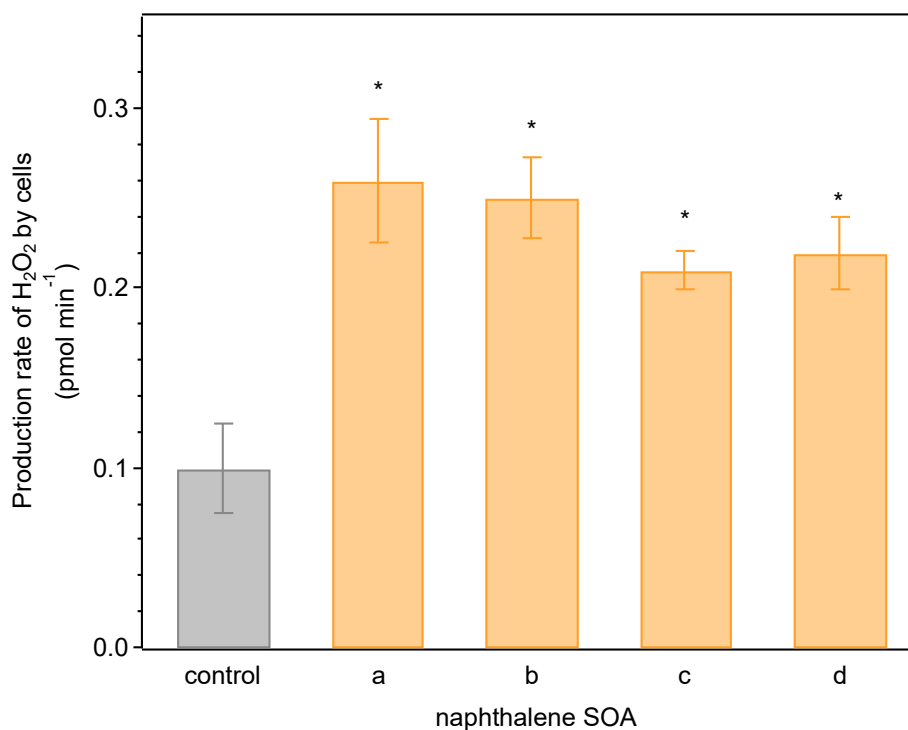


**Figure 3-D.** H<sub>2</sub>O<sub>2</sub> produced by cells after exposure to naphthalene SOA samples (a, b, c, d) or supplemented media (control) for 24 h. The amount of H<sub>2</sub>O<sub>2</sub> produced was quantified using Amplex red. Data are presented as mean ± SE of measurements carried out in triplicate. Statistically significant differences calculated with the *t*-test corresponded to \**p* = 0.01, \**p* = 0.01, \**p* = 0.01 and \**p* = 0.02 for samples a, b, c and d compared to control, respectively.

### 3.3.3 *H<sub>2</sub>O<sub>2</sub> from naphthalene SOA samples and from cells were responsible for the carboxy-DCF fluorescence*

The quantification of H<sub>2</sub>O<sub>2</sub> produced by cells (H<sub>2</sub>O<sub>2</sub>[cells]) and by naphthalene SOA samples interacting with the extraction solution (H<sub>2</sub>O<sub>2</sub>[SOA]) confirmed that both sources contributed to the oxidation of the probe compound (Figure 3-F). For instance, H<sub>2</sub>O<sub>2</sub>[cells] was found to range from 3.02 ± 0.01 to 3.74 ± 0.03 μM H<sub>2</sub>O<sub>2</sub>, which corresponds to a H<sub>2</sub>O<sub>2</sub> yield of 1.03-1.27 ng/μg. H<sub>2</sub>O<sub>2</sub>[SOA] (3.16-4.20 ng/μg) was also quantified in naphthalene SOA samples and was found to be higher than H<sub>2</sub>O<sub>2</sub>[cells]. Additionally, it was shown that H<sub>2</sub>O<sub>2</sub>[SOA] is stable over time and that it can rapidly diffuse into the cells. Therefore, H<sub>2</sub>O<sub>2</sub>[SOA] contributed to the intracellular oxidation of carboxy-H<sub>2</sub>DCF to a greater extent than H<sub>2</sub>O<sub>2</sub>[cells].

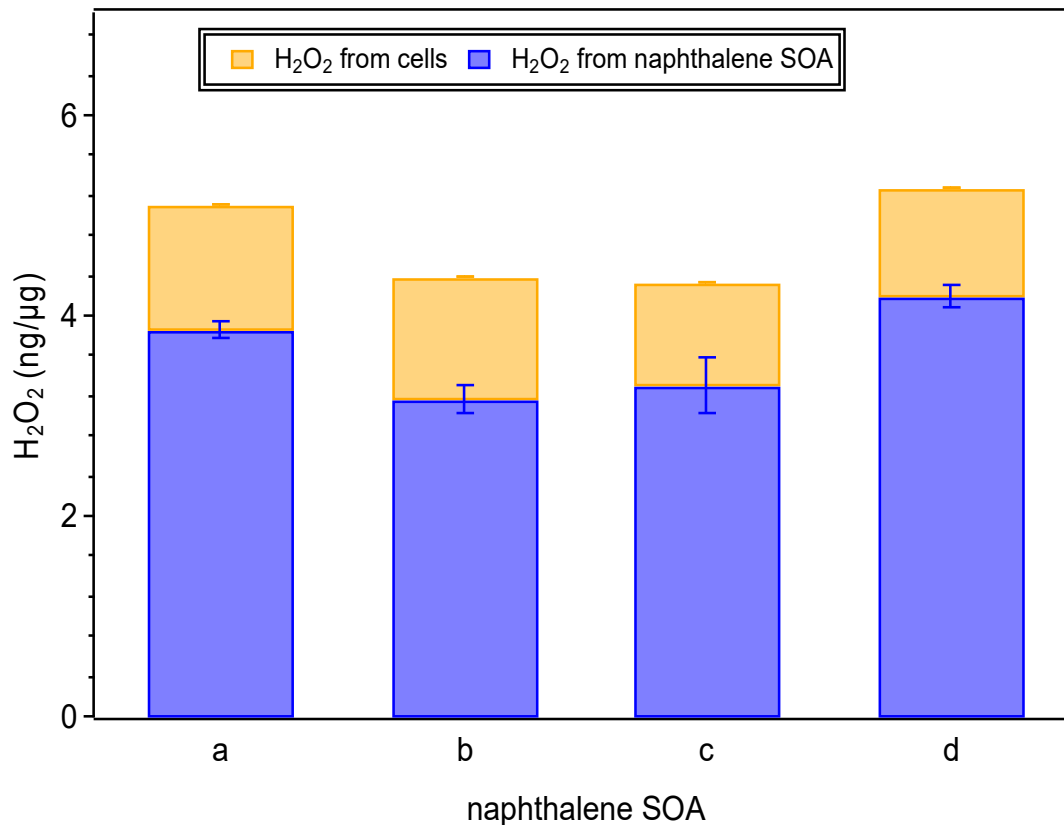


**Figure 3-E. Sources of H<sub>2</sub>O<sub>2</sub> responsible for carboxy-H<sub>2</sub>DCF fluorescence. H<sub>2</sub>O<sub>2</sub><sub>[SOA]</sub> (blue) corresponded to the quantified H<sub>2</sub>O<sub>2</sub> using Amplex red in the absence of cells. H<sub>2</sub>O<sub>2</sub><sub>[cell]</sub> (orange) was estimated by multiplying the rate of H<sub>2</sub>O<sub>2</sub> produced after 24 h exposure to naphthalene SOA samples (measured with Amplex red as well) by the entire exposure period (i.e., 24 h). Values represent mean ± SE of measurements carried out in triplicate.**



## CHAPTER 4. CONCLUSIONS, IMPLICATIONS AND FUTURE WORK

In this study, the general oxidative stress marker carboxy-H<sub>2</sub>DCFDA was used to investigate the contribution of H<sub>2</sub>O<sub>2</sub> to the intracellular generation of ROS/RNS induced by naphthalene SOA exposure. Despite the lack of specificity of carboxy-H<sub>2</sub>DCF,<sup>130</sup> in this study it was shown that the collective use of catalase with this probe can elucidate the role of H<sub>2</sub>O<sub>2</sub> in the mediation of naphthalene SOA-induced cellular responses.

Results in this study showed that the ROS/RNS signal induced by exposure to naphthalene SOA was inhibited by the addition of catalase. Although the probe compound can be oxidized by multiple ROS/RNS,<sup>64</sup> the selective role of catalase in removing H<sub>2</sub>O<sub>2</sub> confirmed that H<sub>2</sub>O<sub>2</sub> was the main ROS present in our system that could oxidize carboxy-H<sub>2</sub>DCF. Furthermore, it was demonstrated that cells exposed to naphthalene SOA samples produced H<sub>2</sub>O<sub>2</sub> ranging from  $0.21 \pm 0.01$  to  $0.26 \pm 0.03$  pmol/min/10<sup>4</sup> cells. Altogether, these results showed that H<sub>2</sub>O<sub>2</sub> was the main ROS generated by the cells upon exposure to naphthalene SOA. These findings contribute to the understanding of the types of ROS/RNS that are generated upon exposure to PM by showing that H<sub>2</sub>O<sub>2</sub> was the mediator of cellular responses induced by naphthalene SOA. This knowledge can motivate future studies to consider different cellular pathways that directly generate H<sub>2</sub>O<sub>2</sub> in order to understand local and systemic effects induced by exposure to naphthalene SOA. Although naphthalene was the only precursor investigated in this study, it is representative of PAH compounds, which have been found in inhalable ambient particles.<sup>89,90</sup> In these terms, results in this study are

relevant for human daily exposure and imply that ambient PM with contents of PAHs could also induce cells to generate H<sub>2</sub>O<sub>2</sub>.

It should be noted that experimental conditions in the generation of PM samples largely influence SOA composition and ROS yields, which can induce different cellular responses. For instance, the expected presence of acidic species and peroxides in naphthalene SOA formed in the absence of NO<sub>x</sub><sup>93</sup> was shown to induce greater ROS/RNS response,<sup>74</sup> which can include other ROS/RNS besides H<sub>2</sub>O<sub>2</sub>. Thus, the dominant role of H<sub>2</sub>O<sub>2</sub> in the mediation of cellular responses found in this study is only applicable for naphthalene SOA formed in the presence of NO<sub>x</sub> and might not be generalized for other systems. Future studies investigating the contribution of H<sub>2</sub>O<sub>2</sub> to the intracellular ROS/RNS response induced by different SOA systems and ambient PM samples are warranted.

Results in this study also showed that H<sub>2</sub>O<sub>2</sub> produced by cells (H<sub>2</sub>O<sub>2</sub>[cells]) and by naphthalene SOA samples interacting with the extraction solution (H<sub>2</sub>O<sub>2</sub>[SOA]) can both contribute to the intracellular oxidation of H<sub>2</sub>DCF. Overall, H<sub>2</sub>O<sub>2</sub>[SOA] (3.16-4.20 ng/μg) was found to be higher than H<sub>2</sub>O<sub>2</sub>[cells] (1.03-1.27 ng/μg). Additionally, it was shown that H<sub>2</sub>O<sub>2</sub>[SOA] is stable over time and that it can rapidly diffuse into the cells. Therefore, H<sub>2</sub>O<sub>2</sub>[SOA] contributed to the intracellular oxidation of carboxy-H<sub>2</sub>DCF to a greater extent than H<sub>2</sub>O<sub>2</sub>[cells]. This suggest that the diffusion of H<sub>2</sub>O<sub>2</sub>[SOA] into the cells represent one of the pathways in which exposure to naphthalene SOA leads to oxidative stress.

## APPENDIX A.

**Table A- 1. Experimental conditions and elemental composition of naphthalene SOA formed in the presence of NO<sub>x</sub>**

<i>Sample</i>	<i>Naphthalene</i>	<i>Relative humidity</i>	<i>SOA mass<sup>a</sup></i>	<i>Initial NO</i>	<i>Initial NO<sub>2</sub></i>	<i>O:C ratio</i>	<i>H:C ratio</i>	<i>N:C ratio</i>	<i>OSc</i>
	<i>ppb</i>	<i>%</i>	<i>μg m<sup>-3</sup></i>	<i>ppb</i>	<i>ppb</i>				
a	222	< 5 %	213	229	392	0.30	0.96	0.010	-0.36
b	321	< 5 %	430	245	471	0.28	0.97	0.009	-0.40
c	450	< 5 %	596	225	333	0.29	0.98	0.009	-0.39
d	550	< 5 %	492	236	401	0.25	0.98	0.007	-0.48

<sup>a</sup> The total aerosol mass collected on filters was calculated by integrating the aerosol volume concentration data from the SMPS over the sampling period and multiplying by the total volume of air collected, as described in Tuet et al.<sup>159</sup> SMPS volume concentrations were converted to mass concentrations by assuming a density of 1.48 g cm<sup>-3</sup> based on prior experiments.<sup>93</sup>

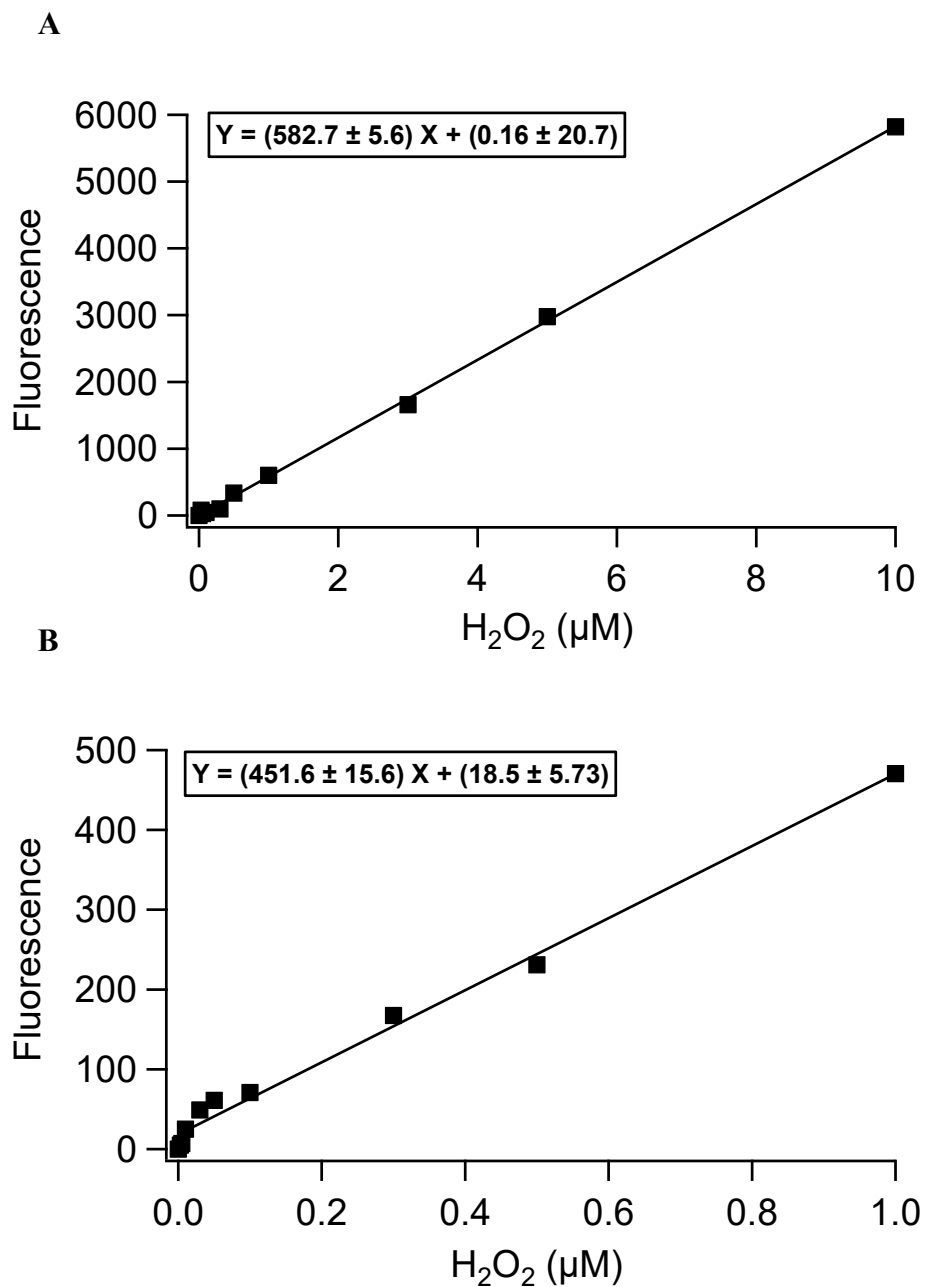


**Figure A- 1. Calibration curve for  $H_2O_2$  (in PBS) for the quantification of  $H_2O_2$  in naphthalene SOA samples (A) and released by cells (B) using Amplex red. Reactions containing Amplex red reagent, Horseradish peroxidase (HRP) and indicated amount of  $H_2O_2$  were incubated for 10 to 30 minutes before measuring fluorescence intensity. Values were corrected for background by subtracting the fluorescence signal from the control sample (0  $\mu M$   $H_2O_2$ ).**

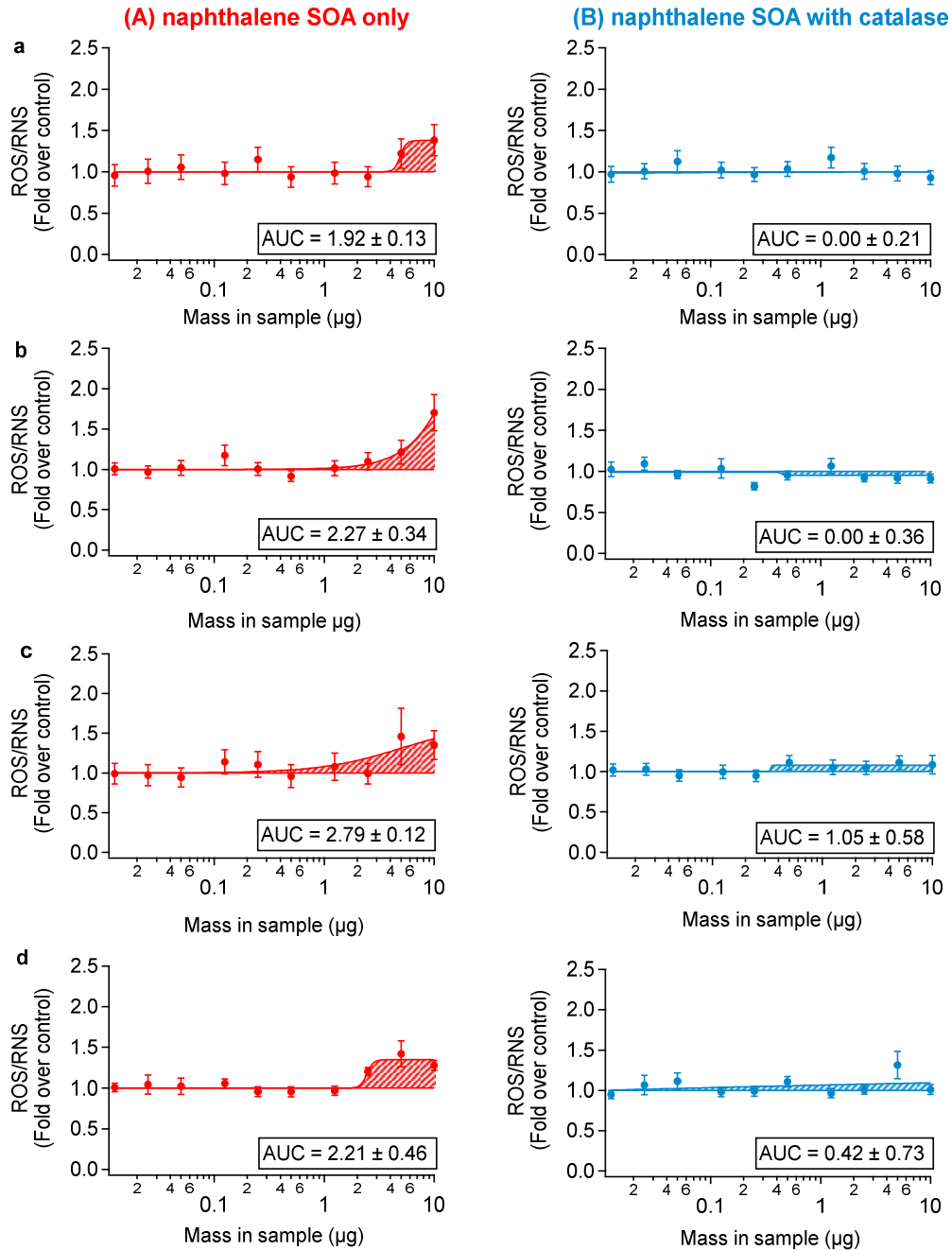


**Figure A-2. Dose-response curve of ROS/RNS produced by exposure to naphthalene SOA (samples a-d). Cells were exposed to naphthalene SOA extracts (A) and naphthalene SOA extracts + 50 U mL<sup>-1</sup> catalase (B) for 24 h. ROS/RNS was calculated using carboxy-H<sub>2</sub>DCFDA. Values represent the fold of change over control cells. Data are presented as means  $\pm$  SE of experiments carried out in triplicate. Every 10-dilution data was fitted with a dose-response curve as described in<sup>74</sup>. AUC data represent means  $\pm$  SE estimated from 3 dose-response fitted curves on each experiment.**

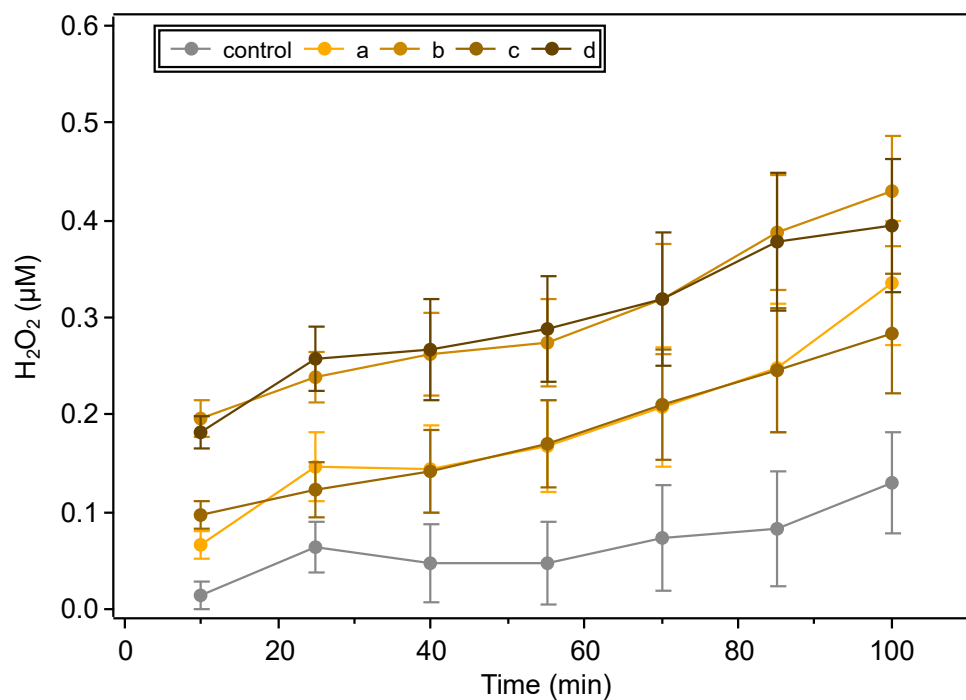


**Figure A- 3. Quantification of H<sub>2</sub>O<sub>2</sub> produced from cells. The cells were first exposed to naphthalene SOA for 24 h. Afterwards, the fluorescence signal was measured every 15 minutes over 100 min using Amplex red. Cells were exposed to naphthalene SOA samples (orange) or supplemented media (grey) for 24 h. Values are presented as mean  $\pm$  SE of experiments carried out in triplicate. H<sub>2</sub>O<sub>2</sub> concentrations were calculated based on the calibration curves shown in Figure A-1.**

## REFERENCES

- (1) Harrabi, I.; Rondeau, V.; Dartigues, J.-F.; Tessier, J.-F.; Filleul, L. Effects of Particulate Air Pollution on Systolic Blood Pressure: A Population-Based Approach. *Environ. Res.* **2006**, *101* (1), 89–93. <https://doi.org/10.1016/j.envres.2006.01.012>.
- (2) Baumgartner, J.; Schauer, J. J.; Ezzati, M.; Lu, L.; Cheng, C.; Patz, J. A.; Bautista, L. E. Indoor Air Pollution and Blood Pressure in Adult Women Living in Rural China. In *Environmental Health Perspectives*; Solomon, S., Qin, D., Manning, M., Chen, Z., Marquis, M., Averyt, K. B., Tignor, M., Miller, H. L., Eds.; Brogan & Partners, 2012; Vol. 119, pp 1390–1395.
- (3) Du, Y.; Xu, X.; Chu, M.; Guo, Y.; Wang, J. Air Particulate Matter and Cardiovascular Disease: The Epidemiological, Biomedical and Clinical Evidence. *J. Thorac. Dis.* **2016**, *8* (1), E8–E19. <https://doi.org/10.3978/j.issn.2072-1439.2015.11.37>.
- (4) Tecer, L. H.; Alagha, O.; Karaca, F.; Tuncel, G.; Eldes, N. Particulate Matter (PM<sub>2.5</sub>, PM<sub>10-2.5</sub>, and PM<sub>10</sub>) and Children’s Hospital Admissions for Asthma and Respiratory Diseases: A Bidirectional Case-Crossover Study. *J. Toxicol. Environ. Heal. - Part A Curr. Issues* **2008**, *71* (8), 512–520. <https://doi.org/10.1080/15287390801907459>.
- (5) Hacon, S.; Ornelas, C.; Ignotti, E.; Longo, K. Fine Particulate Air Pollution and Hospital Admission for Respiratory Diseases in the Amazon Region. *Epidemiology* **2007**, *18* (Suppl), S81. <https://doi.org/10.1097/01.ede.0000288970.67189.c8>.
- (6) Breton, C. V.; Salam, M. T.; Wang, X.; Byun, H.; Siegmund, K. D.; Gilliland, F. D. Particulate Matter, DNA Methylation in Nitric Oxide Synthase, and Childhood Respiratory Disease. **2012**, *120* (9), 1320–1326.
- (7) Peters, A.; Veronesi, B.; Calderón-Garcidueñas, L.; Gehr, P.; Chen, L. C.; Geiser, M.; Reed, W.; Rothen-Rutishauser, B.; Schürch, S.; Schulz, H. Translocation and Potential Neurological Effects of Fine and Ultrafine Particles a Critical Update. *Part. Fibre Toxicol.* **2006**, *3*, 1–13. <https://doi.org/10.1186/1743-8977-3-13>.
- (8) Loane, C.; Pilinis, C.; Lekkas, T. D.; Politis, M. Ambient Particulate Matter and Its Potential Neurological Consequences. *Rev. Neurosci.* **2013**, *24* (3), 323–335. <https://doi.org/10.1515/revneuro-2013-0001>.
- (9) Jung, C. R.; Lin, Y. T.; Hwang, B. F. Ozone, Particulate Matter, and Newly Diagnosed Alzheimer’s Disease: A Population-Based Cohort Study in Taiwan. *J. Alzheimer’s Dis.* **2015**, *44* (2), 573–584. <https://doi.org/10.3233/JAD-140855>.
- (10) Forouzanfar, M. H.; Afshin, A.; Alexander, L. T.; Biryukov, S.; Brauer, M.; Cercy, K.; Charlson, F. J.; Cohen, A. J.; Dandona, L.; Estep, K.; et al. Global, Regional,

and National Comparative Risk Assessment of 79 Behavioural, Environmental and Occupational, and Metabolic Risks or Clusters of Risks, 1990–2015: A Systematic Analysis for the Global Burden of Disease Study 2015. *Lancet* **2016**, *388* (10053), 1659–1724. [https://doi.org/10.1016/S0140-6736\(16\)31679-8](https://doi.org/10.1016/S0140-6736(16)31679-8).

- (11) Miri, M.; Alahabadi, A.; Ehrampush, M. H.; Rad, A.; Lotfi, M. H.; Sheikhha, M. H.; Sakhvidi, M. J. Z. Mortality and Morbidity Due to Exposure to Ambient Particulate Matter. *Ecotoxicol. Environ. Saf.* **2018**, *165* (September), 307–313. <https://doi.org/10.1016/j.ecoenv.2018.09.012>.
- (12) Li, M. H.; Fan, L. C.; Mao, B.; Yang, J. W.; Choi, A. M. K.; Cao, W. J.; Xu, J. F. Short-Term Exposure to Ambient Fine Particulate Matter Increases Hospitalizations and Mortality in COPD: A Systematic Review and Meta-Analysis. *Chest* **2016**, *149* (2), 447–458. <https://doi.org/10.1378/chest.15-0513>.
- (13) R., C.; P., Y.; X., M.; L., W.; C., L.; Y., N.; Y., L.; J., L.; J., Q.; J., Y.; et al. Associations between Coarse Particulate Matter Air Pollution and Cause-Specific Mortality: A Nationwide Analysis in 272 Chinese Cities. *Environ. Health Perspect.* **2019**, *127* (1), 17008-1–9. <https://doi.org/10.1289/EHP2711>.
- (14) Burnett, R.; Chen, H.; Szyszkowicz, M.; Fann, N.; Hubbell, B.; Pope, C. A.; Apte, J. S.; Brauer, M.; Cohen, A.; Weichenthal, S.; et al. Global Estimates of Mortality Associated with Long-Term Exposure to Outdoor Fine Particulate Matter. *Proc. Natl. Acad. Sci.* **2018**, *115* (38), 9592–9597. <https://doi.org/10.1073/pnas.1803222115>.
- (15) Pardo, M.; Xu, F.; Qiu, X.; Zhu, T.; Rudich, Y. Seasonal Variations in Fine Particle Composition from Beijing Prompt Oxidative Stress Response in Mouse Lung and Liver. *Sci. Total Environ.* **2018**, *626*, 147–155. <https://doi.org/10.1016/j.scitotenv.2018.01.017>.
- (16) Wang, X.; Moraes, C. T. Increases in Mitochondrial Biogenesis Impair Carcinogenesis at Multiple Levels. *Mol. Oncol.* **2011**, *5* (5), 399–409. <https://doi.org/10.1016/j.molonc.2011.07.008>.
- (17) Magnani, N. D.; Muresan, X. M.; Belmonte, G.; Cervellati, F.; Sticozzi, C.; Pecorelli, A.; Miracco, C.; Marchini, T.; Evelson, P.; Valacchi, G. Skin Damage Mechanisms Related to Airborne Particulate Matter Exposure. *Toxicol. Sci.* **2016**, *149* (1), 227–236. <https://doi.org/10.1093/toxsci/kfv230>.
- (18) Budinger, G. R. S.; McKell, J. L.; Urich, D.; Foiles, N.; Weiss, I.; Chiarella, S. E.; Gonzalez, A.; Soberanes, S.; Ghio, A. J.; Nigdelioglu, R.; et al. Particulate Matter-Induced Lung Inflammation Increases Systemic Levels of PAI-1 and Activates Coagulation through Distinct Mechanisms. *PLoS One* **2011**, *6* (4), 1–9. <https://doi.org/10.1371/journal.pone.0018525>.
- (19) Guan, L.; Geng, X.; Stone, C.; Cosky, E. E. P.; Ji, Y.; Du, H.; Zhang, K.; Sun, Q.; Ding, Y. PM 2.5 Exposure Induces Systemic Inflammation and Oxidative Stress in



an Intracranial Atherosclerosis Rat Model. *Environ. Toxicol.* **2019**, *34* (4), 530–538. <https://doi.org/10.1002/tox.22707>.

- (20) Ralph J. Delfino, Norbert Staimer, Thomas Tjoa, Mohammad Arhamib, C.; Andrea; Polidorib, Daniel L. Gillend, Steven C. George, M. M. S.; Schauer, J. J.; And; Sioutas, C. Associations of Primary and Secondary Organic Aerosols With Airway and Systemic Inflammation in an Elderly Panel Cohort. *Epidemiology* **2010**, *21* (6), doi:10.1097/EDE.0b013e3181f20e6c. <https://doi.org/10.1097/EDE.0b013e3181f20e6c>.Associations.
- (21) Ohnishi, S.; Hiraku, Y.; Hasegawa, K.; Hirakawa, K.; Oikawa, S.; Murata, M.; Kawanishi, S. Mechanism of Oxidative DNA Damage Induced by Metabolites of Carcinogenic Naphthalene. *Mutat. Res. - Genet. Toxicol. Environ. Mutagen.* **2018**, *827* (January), 42–49. <https://doi.org/10.1016/j.mrgentox.2018.01.005>.
- (22) Akhtar, U. S.; McWhinney, R. D.; Rastogi, N.; Abbatt, J. P. D.; Evans, G. J.; Scott, J. A. Cytotoxic and Proinflammatory Effects of Ambient and Source-Related Particulate Matter (PM) in Relation to the Production of Reactive Oxygen Species (ROS) and Cytokine Adsorption by Particles. *Inhal. Toxicol.* **2010**, *22* (SUPPL. 2), 37–47. <https://doi.org/10.3109/08958378.2010.518377>.
- (23) Pardo, M.; Shafer, M. M.; Rudich, A.; Schauer, J. J.; Rudich, Y. Single Exposure to near Roadway Particulate Matter Leads to Confined Inflammatory and Defense Responses: Possible Role of Metals. *Environ. Sci. Technol.* **2015**, *49* (14), 8777–8785. <https://doi.org/10.1021/acs.est.5b01449>.
- (24) Peixoto, M. S.; de Oliveira Galvão, M. F.; Batistuzzo de Medeiros, S. R. Cell Death Pathways of Particulate Matter Toxicity. *Chemosphere* **2017**, *188*, 32–48. <https://doi.org/10.1016/j.chemosphere.2017.08.076>.
- (25) Shuster-Meiseles, T.; Shafer, M. M.; Heo, J.; Pardo, M.; Antkiewicz, D. S.; Schauer, J. J.; Rudich, A.; Rudich, Y. ROS-Generating/ARE-Activating Capacity of Metals in Roadway Particulate Matter Deposited in Urban Environment. *Environ. Res.* **2016**, *146*, 252–262. <https://doi.org/10.1016/j.envres.2016.01.009>.
- (26) Borm, P. J. A.; Kelly, F.; Künzli, N.; Schins, R. P. F.; Donaldson, K. Oxidant Generation by Particulate Matter: From Biologically Effective Dose to a Promising, Novel Metric. *Occup. Environ. Med.* **2007**, *64* (2), 73–74. <https://doi.org/10.1136/oem.2006.029090>.
- (27) Ghio, A. J.; Carraway, M. S.; Madden, M. C. Composition of Air Pollution Particles and Oxidative Stress in Cells, Tissues, and Living Systems. *J. Toxicol. Environ. Heal. - Part B Crit. Rev.* **2012**, *15* (1), 1–21. <https://doi.org/10.1080/10937404.2012.632359>.
- (28) Scherz-Shouval, R.; Elazar, Z. ROS, Mitochondria and the Regulation of Autophagy. *Trends Cell Biol.* **2007**, *17* (9), 422–427. <https://doi.org/10.1016/j.tcb.2007.07.009>.

- (29) Schieber, M.; Chandel, N. S. ROS Function in Redox Signaling and Oxidative Stress. *Curr. Biol.* **2014**, *24* (10), R453–R462. <https://doi.org/10.1016/j.cub.2014.03.034>.
- (30) Orrenius, S. Reactive Oxygen Species in Mitochondria-Mediated Cell Death. *Drug Metab. Rev.* **2007**, *39* (2–3), 443–455. <https://doi.org/10.1080/03602530701468516>.
- (31) Dröge, W. Free Radicals in the Physiological Control of Cell Function. *Physiol. Rev.* **2002**, *82* (1), 47–95. <https://doi.org/10.1152/physrev.00018.2001>.
- (32) Forman, H. J.; Torres, M. Reactive Oxygen Species and Cell Signaling. *Am. J. Respir. Cell Mol. Biol.* **2001**, *25* (6), 661–663. <https://doi.org/10.1165/ajrcmb.25.6.f213>.
- (33) Valko, M.; Leibfritz, D.; Moncol, J.; Cronin, M. T. D.; Mazur, M.; Telser, J. Free Radicals and Antioxidants in Normal Physiological Functions and Human Disease. *Int. J. Biochem. Cell Biol.* **2007**, *39* (1), 44–84. <https://doi.org/10.1016/j.biocel.2006.07.001>.
- (34) Marcadenti, A.; Lopes Assis Coelho, C. Dietary Antioxidant and Oxidative Stress: Interaction between Vitamins and Genetics. *J. Nutr. Heal. Food Sci.* **2015**, *3* (1). <https://doi.org/10.15226/jnhfs.2015.00138>.
- (35) Finkel, T. Critical Review Reactive Oxygen Species and Signal Transduction. *IUBMB Life* **2001**, *52*, 3–6.
- (36) Sies, H. Role of Metabolic H<sub>2</sub>O<sub>2</sub> Generation. *J. Biol. Chem.* **2014**, *289* (13), 8735–8741. <https://doi.org/10.1074/jbc.R113.544635>.
- (37) Sies, H. Hydrogen Peroxide as a Central Redox Signaling Molecule in Physiological Oxidative Stress: Oxidative Eustress. *Redox Biol.* **2017**, *11* (January), 613–619. <https://doi.org/10.1016/j.redox.2016.12.035>.
- (38) Veal, E. A.; Day, A. M.; Morgan, B. A. Hydrogen Peroxide Sensing and Signaling. **2007**, 1–14. <https://doi.org/10.1016/j.molcel.2007.03.016>.
- (39) Rhee, S. G. Hydrogen Peroxide, a Necessary Evil for Cell Signaling. *Science* (80-). **2006**, *312* (June), 1882–1884.
- (40) Go, Y. M.; Chandler, J. D.; Jones, D. P. The Cysteine Proteome. *Free Radic. Biol. Med.* **2015**, *84*, 227–245. <https://doi.org/10.1016/j.freeradbiomed.2015.03.022>.
- (41) Blake, D. R.; Allen, R. E.; Lunec, J. Free Radicals in Biological Systems: A Review Orientated to Inflammatory Processes. **1987**, *43* (2), 371–385.
- (42) Sies, H. Biochemistry of the Peroxisome in the Liver Cell. *Angew. Chemie Int. Ed. English* **1974**, *13* (11), 706–718. <https://doi.org/10.1002/anie.197407061>.

- (43) Bowie, A.; O'Neill, L. A. . Oxidative Stress and Nuclear Factor-KB Activation. *Biochem. Pharmacol.* **2002**, *59* (1), 13–23. [https://doi.org/10.1016/s0006-2952\(99\)00296-8](https://doi.org/10.1016/s0006-2952(99)00296-8).
- (44) Lennicke, C.; Rahn, J.; Lichtenfels, R.; Wessjohann, L. A.; Seliger, B. Hydrogen Peroxide – Production , Fate and Role in Redox Signaling of Tumor Cells. *Cell Commun. Signal.* **2015**, 1–19. <https://doi.org/10.1186/s12964-015-0118-6>.
- (45) Pelicano, H.; Carney, D.; Huang, P. ROS Stress in Cancer Cells and Therapeutic Implications. *Drug Resist. Updat.* **2004**, *7* (2), 97–110. <https://doi.org/10.1016/j.drug.2004.01.004>.
- (46) Mittal, M.; Siddiqui, M. R.; Tran, K.; Reddy, S. P.; Malik, A. B. Reactive Oxygen Species in Inflammation and Tissue Injury. *Antioxid. Redox Signal.* **2014**, *20* (7), 1126–1167. <https://doi.org/10.1089/ars.2012.5149>.
- (47) Finkel, T. Signal Transduction by Mitochondrial Oxidants. *J. Biol. Chem.* **2012**, *287* (7), 4434–4440. <https://doi.org/10.1074/jbc.R111.271999>.
- (48) Ott, M.; Gogvadze, V.; Orrenius, S.; Zhivotovsky, B. Mitochondria, Oxidative Stress and Cell Death. *Apoptosis* **2007**, *12* (5), 913–922. <https://doi.org/10.1007/s10495-007-0756-2>.
- (49) Birben, E.; Sahiner, U. M.; Sackesen, C.; Erzurum, S.; Kalayci, O. Oxidative Stress and Antioxidant Defense. *World Allergy Organ. J.* **2012**, 10–19.
- (50) Li, Z.; Hyseni, X.; Carter, J. D.; Soukup, J. M.; Dailey, L. A.; Huang, Y.-C. T. Pollutant Particles Enhanced H<sub>2</sub>O<sub>2</sub> Production from NAD(P)H Oxidase and Mitochondria in Human Pulmonary Artery Endothelial Cells . *Am. J. Physiol. Physiol.* **2006**, *291* (2), C357–C365. <https://doi.org/10.1152/ajpcell.00365.2005>.
- (51) Knaapen, A. M.; Shi, T.; Borm, P. J. A.; Schins, R. P. F. Soluble Metals as Well as the Insoluble Particle Fraction Are Involved in Cellular DNA Damage Induced by Particulate Matter. *Mol. Cell. Biochem.* **2002**, *234–235*, 317–326. <https://doi.org/10.1023/A:1015970023889>.
- (52) Huang, Y. C. T.; Li, Z.; Carter, J. D.; Soukup, J. M.; Schwartz, D. A.; Yang, I. V. Fine Ambient Particles Induce Oxidative Stress and Metal Binding Genes in Human Alveolar Macrophages. *Am. J. Respir. Cell Mol. Biol.* **2009**, *41* (5), 544–552. <https://doi.org/10.1165/rcmb.2008-0064OC>.
- (53) Morio, L. A.; Hooper, K. A.; Brittingham, J.; Li, T. H.; Gordon, R. E.; Turpin, B. J.; Laskin, D. L. Tissue Injury Following Inhalation of Fine Particulate Matter and Hydrogen Peroxide Is Associated with Altered Production of Inflammatory Mediators and Antioxidants by Alveolar Macrophages. *Toxicol. Appl. Pharmacol.* **2001**, *177* (3), 188–199. <https://doi.org/10.1006/taap.2001.9316>.
- (54) Maeda, H.; Matsu-ura, S.; Nishida, M.; Yamauchi, Y.; Ohmori, H. Assessment of

- Acyl Groups and Reaction Conditions in the Competition between Perhydrolysis and Hydrolysis of Acyl Resorufins for Developing an Indicator Reaction for Fluorometric Analysis of Hydrogen Peroxide. *Chem. Pharm. Bull. (Tokyo)*. **2002**, *50* (2), 169–174. <https://doi.org/10.1248/cpb.50.169>.
- (55) Xu, J.; Zhang, Y.; Yu, H.; Gao, X.; Shao, S. Mitochondria-Targeted Fluorescent Probe for Imaging Hydrogen Peroxide in Living Cells. *Anal. Chem.* **2016**, *88* (2), 1455–1461. <https://doi.org/10.1021/acs.analchem.5b04424>.
- (56) Chang, M. C. Y.; Pralle, A.; Isacoff, E. Y.; Chang, C. J. A Selective, Cell-Permeable Optical Probe for Hydrogen Peroxide in Living Cells. *J. Am. Chem. Soc.* **2004**, *126* (47), 15392–15393. <https://doi.org/10.1021/ja0441716>.
- (57) Srikun, D.; Miller, E. W.; Domaille, D. W.; Chang, C. J. An ICT-Based Approach to Ratiometric Fluorescence Imaging of Hydrogen Peroxide Produced in Living Cells Duangkhae Srikun, Evan W. Miller, Dylan W. Domaille, and Christopher J. Chang\*. *Technology* **2008**, *60* (6 mL), 8–11.
- (58) Soh, N. Recent Advances in Fluorescent Probes for the Detection of Reactive Oxygen Species. *Anal. Bioanal. Chem.* **2006**, *386* (3), 532–543. <https://doi.org/10.1007/s00216-006-0366-9>.
- (59) Pardo, M.; Porat, Z.; Rudich, A.; Schauer, J. J.; Rudich, Y. Repeated Exposures to Roadside Particulate Matter Extracts Suppresses Pulmonary Defense Mechanisms, Resulting in Lipid and Protein Oxidative Damage. *Environ. Pollut.* **2016**, *210*, 227–237. <https://doi.org/10.1016/j.envpol.2015.12.009>.
- (60) Landreman, A. P.; Shafer, M. M.; Hemming, J. C.; Michael, P.; Schauer, J. J.; Prash, A.; Shafer, M. M.; Hemming, J. C.; Landreman, A. P.; Shafer, M. M.; et al. A Macrophage-Based Method for the Assessment of the Reactive Oxygen Species ( ROS ) Activity of Atmospheric Particulate Matter ( PM ) and Application to Routine ( Daily-24 h ) Aerosol Monitoring Studies A Macrophage-Based Method for the Assessment of The . **2008**, *6826* (April 2017). <https://doi.org/10.1080/02786820802363819>.
- (61) Kroll, A.; Gietl, J. K.; Wiesmuller, G. A.; Gonsel, A.; Wohlleben, W.; Schneckeburguer, J.; Klemm, O. In Vitro Toxicology of Ambient Particulate Matter: Correlation of Cellular Effects with Particle Size and Components. *Environ. Toxicol.* **2010**, *28* (2), 76–86. <https://doi.org/10.1002/tox>.
- (62) Baulig, A.; Sourdeval, M.; Meyer, M.; Marano, F.; Baeza-Squiban, A. Biological Effects of Atmospheric Particles on Human Bronchial Epithelial Cells. Comparison with Diesel Exhaust Particles. *Toxicol. Vitr.* **2003**, *17* (5–6), 567–573. [https://doi.org/10.1016/S0887-2333\(03\)00115-2](https://doi.org/10.1016/S0887-2333(03)00115-2).
- (63) Brandt, R.; Keston, A. S. Synthesis of Diacetyldichlorofluorescein : A Stable Reagent for Fluorometric Analysis. **1965**, No. C, 6–9.

- (64) Chen, X.; Zhong, Z.; Xu, Z.; Chen, L.; Wang, Y. 2',7'-Dichlorodihydrofluorescein as a Fluorescent Probe for Reactive Oxygen Species Measurement: Forty Years of Application and Controversy. *Free Radic. Res.* **2010**, *44* (6), 587–604. <https://doi.org/10.3109/10715761003709802>.
- (65) Hiura, T. S.; Li, N.; Kaplan, R.; Horwitz, M.; Seagrave, J.-C.; Nel, A. E. The Role of a Mitochondrial Pathway in the Induction of Apoptosis by Chemicals Extracted from Diesel Exhaust Particles. *J. Immunol.* **2000**, *165* (5), 2703–2711. <https://doi.org/10.4049/jimmunol.165.5.2703>.
- (66) Li, N.; Wang, M.; Oberley, T. D.; Sempf, J. M.; Nel, A. E. Comparison of the Pro-Oxidative and Proinflammatory Effects of Organic Diesel Exhaust Particle Chemicals in Bronchial Epithelial Cells and Macrophages. *J. Immunol.* **2002**, *169* (8), 4531–4541. <https://doi.org/10.4049/jimmunol.169.8.4531>.
- (67) Hiura, T. S.; Kaszubowski, M. P.; Li, N.; Nel, A. E. Chemicals in Diesel Exhaust Particles Generate Reactive Oxygen Radicals and Induce Apoptosis in Macrophages. *J. Immunol.* **1999**, *163* (10), 5582–5591.
- (68) Yi, S.; Zhang, F.; Qu, F.; Ding, W. Water-Insoluble Fraction of Airborne Particulate Matter (PM10) Induces Oxidative Stress in Human Lung Epithelial A549 Cells. *Environ. Toxicol.* **2014**, *29* (2), 226–233. <https://doi.org/10.1002/tox>.
- (69) Wrona, M.; Patel, K.; Wardman, P. Reactivity of 2',7'-Dichlorodihydrofluorescein and Dihydrorhodamine 123 and Their Oxidized Forms toward Carbonate, Nitrogen Dioxide, and Hydroxyl Radicals. *Free Radic. Biol. Med.* **2005**, *38* (2), 262–270. <https://doi.org/10.1016/j.freeradbiomed.2004.10.022>.
- (70) Crow, J. P. Dichlorodihydrofluorescein and Dihydrorhodamine 123 Are Sensitive Indicators of Peroxynitrite in Vitro: Implications for Intracellular Measurement of Reactive Nitrogen and Oxygen Species. *Nitric Oxide - Biol. Chem.* **1997**, *1* (2), 145–157. <https://doi.org/10.1006/niox.1996.0113>.
- (71) Jakubowski, W.; Bartosz, G. 2',7'-DICHLOROFLUORESCIN OXIDATION AND REACTIVE OXYGEN SPECIES: WHAT DOES IT MEASURE? **2000**, *24* (10), 757–760. <https://doi.org/10.1006/cbir.2000.0556>.
- (72) Tarpey, M. M.; Fridovich, I. Methods of Detection of Vascular Reactive Species Nitric Oxide, Superoxide, Hydrogen Peroxide, and Peroxynitrite. **2001**, *89* (3), 224–236.
- (73) Piao, M. J.; Ahn, M. J.; Kang, K. A.; Ryu, Y. S.; Hyun, Y. J.; Shilnikova, K.; Zhen, A. X.; Jeong, J. W.; Choi, Y. H.; Kang, H. K.; et al. Particulate Matter 2.5 Damages Skin Cells by Inducing Oxidative Stress, Subcellular Organelle Dysfunction, and Apoptosis. *Arch. Toxicol.* **2018**, *92* (6), 2077–2091. <https://doi.org/10.1007/s00204-018-2197-9>.
- (74) Tuet, W. Y.; Fok, S.; Verma, V.; Tagle Rodriguez, M. S.; Grosberg, A.; Champion,

- J. A.; Ng, N. L. Dose-Dependent Intracellular Reactive Oxygen and Nitrogen Species (ROS/RNS) Production from Particulate Matter Exposure: Comparison to Oxidative Potential and Chemical Composition. *Atmos. Environ.* **2016**, *144*, 335–344. <https://doi.org/10.1016/j.atmosenv.2016.09.005>.
- (75) Shafer, M. M.; Perkins, D. A.; Antkiewicz, D. S.; Stone, E. A.; Quraishi, T. A.; Schauer, J. J. Reactive Oxygen Species Activity and Chemical Speciation of Size-Fractionated Atmospheric Particulate Matter from Lahore, Pakistan: An Important Role for Transition Metals. *J. Environ. Monit.* **2010**, *12* (3), 704–715. <https://doi.org/10.1039/B915008K>.
- (76) Palleschi, S.; Rossi, B.; Armiento, G.; Montereali, M. R.; Nardi, E.; Mazziotti Tagliani, S.; Inglessis, M.; Gianfagna, A.; Silvestroni, L. Toxicity of the Readily Leachable Fraction of Urban PM<sub>2.5</sub> to Human Lung Epithelial Cells: Role of Soluble Metals. *Chemosphere* **2018**, *196*, 35–44. <https://doi.org/10.1016/j.chemosphere.2017.12.147>.
- (77) Verma, V.; Wang, Y.; El-Afifi, R.; Fang, T.; Rowland, J.; Russell, A. G.; Weber, R. J. Fractionating Ambient Humic-like Substances (HULIS) for Their Reactive Oxygen Species Activity - Assessing the Importance of Quinones and Atmospheric Aging. *Atmos. Environ.* **2015**, *120*, 351–359. <https://doi.org/10.1016/j.atmosenv.2015.09.010>.
- (78) Ma, Y.; Cheng, Y.; Qiu, X.; Cao, G.; Fang, Y.; Wang, J.; Zhu, T.; Yu, J.; Hu, D. Sources and Oxidative Potential of Water-Soluble Humic-like Substances in Fine Particulate Matter in Beijing. *Atmos. Chem. Phys.* **2018**, *18* (8), 5607–5617. <https://doi.org/10.5194/acp-18-5607-2018>.
- (79) Tuet, W. Y.; Chen, Y.; Fok, S.; Champion, J. A.; Ng, N. L. Inflammatory Responses to Secondary Organic Aerosols (SOA) Generated from Biogenic and Anthropogenic Precursors. *Atmos. Chem. Phys.* **2017**, *17* (18), 11423–11440. <https://doi.org/10.5194/acp-17-11423-2017>.
- (80) Arashiro, M.; Lin, Y.-H.; Zhang, Z.; Sexton, K. G.; Gold, A.; Jaspers, I.; Fry, R. C.; Surratt, J. D. Effect of Secondary Organic Aerosol from Isoprene-Derived Hydroxyhydroperoxides on the Expression of Oxidative Stress Response Genes in Human Bronchial Epithelial Cells. *Environ. Sci. Process. Impacts* **2018**, *20*, 332–339. <https://doi.org/10.1039/C7EM00439G>.
- (81) Hallquist, M.; Wenger, J. C.; Baltensperger, U.; Rudich, Y.; Simpson, D.; Claeys, M.; Dommen, J.; Donahue, N. M.; George, C.; Goldstein, a. H.; et al. The Formation, Properties and Impact of Secondary Organic Aerosol: Current and Emerging Issues. *Atmos. Chem. Phys.* **2009**, *9* (14), 5155–5236. <https://doi.org/10.5194/acp-9-5155-2009>.
- (82) Jimenez, J. L.; Canagaratna, M. R.; Donahue, N. M.; Prevot, A. S. H.; Zhang, Q.; Kroll, J. H.; DeCarlo, P. F.; Allan, J. D.; Coe, H.; Ng, N. L.; et al. Evolution of Organic Aerosols in the Atmosphere. *Science (80-. )*. **2009**, *326* (5959), 1525–1529.

<https://doi.org/10.1126/science.1180353>.

- (83) Zhang, Q.; Jimenez, J. L.; Canagaratna, M. R.; Allan, J. D.; Coe, H.; Ulbrich, I.; Alfarra, M. R.; Takami, A.; Middlebrook, A. M.; Sun, Y. L.; et al. Ubiquity and Dominance of Oxygenated Species in Organic Aerosols in Anthropogenically-Influenced Northern Hemisphere Midlatitudes. *Geophys. Res. Lett.* **2007**, *34* (13), 1–6. <https://doi.org/10.1029/2007GL029979>.
- (84) Ng, N. L.; Kroll, J. H.; Keywood, M. D.; Bahreini, R.; Varutbangkul, V.; Flagan, R. C.; Seinfeld, J. H.; Lee, A.; Goldstein, A. H. Contribution of First- versus Second-Generation Products to Secondary Organic Aerosols Formed in the Oxidation of Biogenic Hydrocarbons. *Environ. Sci. Technol.* **2006**, *40* (7), 2283–2297. <https://doi.org/10.1021/es052269u>.
- (85) Kanakidou, M.; Seinfeld, J. H.; Pandis, S. N.; Barnes, I.; Dentener, F. J.; Facchini, M. C.; Dingenen, R. V.; Ervens, B.; Nenes, A.; Nielsen, C. J.; et al. Organic Aerosol and Global Climate Modelling: A Review. *Atmos. Chem. Phys.* **2005**, *5* (4), 1053–1123. <https://doi.org/10.5194/acp-5-1053-2005>.
- (86) Seinfeld, J. H.; Pankow, J. F. Organic Atmospheric Particulate Material. *Annu. Rev. Phys. Chem.* **2003**, *54* (1), 121–140. <https://doi.org/10.1146/annurev.physchem.54.011002.103756>.
- (87) Tuet, W. Y.; Chen, Y.; Xu, L.; Fok, S.; Gao, D.; Weber, R. J.; Ng, N. L. Chemical Oxidative Potential of Secondary Organic Aerosol ( SOA ) Generated from the Photooxidation of Biogenic and Anthropogenic Volatile Organic Compounds. **2017**, 839–853. <https://doi.org/10.5194/acp-17-839-2017>.
- (88) McWhinney, R. D.; Zhou, S.; Abbatt, J. P. D. Naphthalene SOA: Redox Activity and Naphthoquinone Gas-Particle Partitioning. *Atmos. Chem. Phys.* **2013**, *13* (19), 9731–9744. <https://doi.org/10.5194/acp-13-9731-2013>.
- (89) Liu, B.; Xue, Z.; Zhu, X.; Jia, C. Long-Term Trends (1990–2014), Health Risks, and Sources of Atmospheric Polycyclic Aromatic Hydrocarbons (PAHs) in the U.S. *Environ. Pollut.* **2017**, *220*, 1171–1179. <https://doi.org/10.1016/j.envpol.2016.11.018>.
- (90) Ravindra, K.; Sokhi, R.; Van Grieken, R. Atmospheric Polycyclic Aromatic Hydrocarbons: Source Attribution, Emission Factors and Regulation. *Atmos. Environ.* **2008**, *42* (13), 2895–2921. <https://doi.org/10.1016/j.atmosenv.2007.12.010>.
- (91) Boyd, C. M.; Sanchez, J.; Xu, L.; Eugene, A. J.; Nah, T.; Tuet, W. Y.; Guzman, M. I.; Ng, N. L. Secondary Organic Aerosol Formation from the  $\beta$ -Pinene+NO<sub>3</sub> System: Effect of Humidity and Peroxy Radical Fate. *Atmos. Chem. Phys.* **2015**, *15* (13), 7497–7522. <https://doi.org/10.5194/acp-15-7497-2015>.
- (92) Tuet, W. Y.; Chen, Y.; Fok, S.; Gao, D.; Weber, R. J.; Champion, J. A.; Ng, N. L.

Chemical and Cellular Oxidant Production Induced by Naphthalene Secondary Organic Aerosol (SOA): Effect of Redox-Active Metals and Photochemical Aging. *Sci. Rep.* **2017**, 7 (1), 1–10. <https://doi.org/10.1038/s41598-017-15071-8>.

- (93) Kautzman, K. E.; Surratt, J. D.; Chan, M. N.; Chan, A. W. H.; Hersey, S. P.; Chhabra, P. S.; Dalleska, N. F.; Wennberg, P. O.; Flagan, R. C.; Seinfeld, J. H. Chemical Composition of Gas- and Aerosol-Phase Products from the Photooxidation of Naphthalene. *Journal of Physical Chemistry A*. 2010, pp 913–934. <https://doi.org/10.1021/jp908530s>.
- (94) Canagaratna, M. R.; Jimenez, J. L.; Kroll, J. H.; Chen, Q.; Kessler, S. H.; Massoli, P.; Hildebrandt Ruiz, L.; Fortner, E.; Williams, L. R.; Wilson, K. R.; et al. Elemental Ratio Measurements of Organic Compounds Using Aerosol Mass Spectrometry: Characterization, Improved Calibration, and Implications. *Atmos. Chem. Phys.* **2015**, 15 (1), 253–272. <https://doi.org/10.5194/acp-15-253-2015>.
- (95) Kroll, J. H.; Donahue, N. M.; Jimenez, J. L.; Kessler, S. H.; Canagaratna, M. R.; Wilson, K. R.; Altieri, K. E.; Mazzoleni, L. R.; Wozniak, A. S.; Bluhm, H.; et al. Carbon Oxidation State as a Metric for Describing the Chemistry of Atmospheric Organic Aerosol. *Nat. Chem.* **2011**, 3 (2), 133–139. <https://doi.org/10.1038/nchem.948>.
- (96) Fang, T.; Verma, V.; Guo, H.; King, L. E.; Edgerton, E. S.; Weber, R. J. A Semi-Automated System for Quantifying the Oxidative Potential of Ambient Particles in Aqueous Extracts Using the Dithiothreitol (DTT) Assay: Results from the Southeastern Center for Air Pollution and Epidemiology (SCAPE). *Atmos. Meas. Tech.* **2015**, 8 (1), 471–482. <https://doi.org/10.5194/amt-8-471-2015>.
- (97) Lyublinskaya, O. G.; Borisov, Y. G.; Pugovkina, N. A.; Smirnova, I. S.; Obidina, J. V.; Ivanova, J. S.; Zenin, V. V.; Shatrova, A. N.; Borodkina, A. V.; Aksenov, N. D.; et al. Reactive Oxygen Species Are Required for Human Mesenchymal Stem Cells to Initiate Proliferation after the Quiescence Exit. *Oxid. Med. Cell. Longev.* **2015**, 2015, 1–8. <https://doi.org/10.1155/2015/502105>.
- (98) Carter, W. O.; Narayanan, P. K.; Robinson, J. P. Intracellular Hydrogen Peroxide and Superoxide Anion Detection in Endothelial Cells. *J. Leukoc. Biol.* **1994**, 55.
- (99) Hagedorn, M.; McCarthy, M.; Carter, V. L.; Meyers, S. A. Oxidative Stress in Zebrafish ( *Danio Rerio* ) Sperm. **2012**, 7 (6), 2–12. <https://doi.org/10.1371/journal.pone.0039397>.
- (100) Mishin, V.; Gray, J. P.; Heck, D. E.; Laskin, D. L.; Laskin, J. D. Free Radical Biology & Medicine Application of the Amplex Red / Horseradish Peroxidase Assay to Measure Hydrogen Peroxide Generation by Recombinant Microsomal Enzymes. *Free Radic. Biol. Med.* **2010**, 48 (11), 1485–1491. <https://doi.org/10.1016/j.freeradbiomed.2010.02.030>.
- (101) Molecular Probes. Amplex ® Red Hydrogen Peroxide / Peroxidase Assay Kit. 2009.



- (102) Tong, H.; Lakey, P. S. J.; Arangio, A. M.; Socorro, J.; Shen, F.; Lucas, K.; Brune, W. H.; Po, U.; Shiraiwa, M. Reactive Oxygen Species Formed by Secondary Organic Aerosols in Water and Surrogate Lung Fluid. **2018**. <https://doi.org/10.1021/acs.est.8b03695>.
- (103) Sebens, S.; Bauer, I.; Geismann, C.; Grage-Griebenow, E.; Ehlers, S.; Kruse, M. L.; Arlt, A.; Schäfer, H. Inflammatory Macrophages Induce Nrf2 Transcription Factor-Dependent Proteasome Activity in Colonic NCM460 Cells and Thereby Confer Anti-Apoptotic Protection. *J. Biol. Chem.* **2011**, *286* (47), 40911–40921. <https://doi.org/10.1074/jbc.M111.274902>.
- (104) Sen, P.; Mukherjee, S.; Bhaumik, G.; Das, P. Enhancement of Catalase Activity by Repetitive Low-Grade H<sub>2</sub>O<sub>2</sub> Exposures Protects Fibroblasts from Subsequent Stress-Induced Apoptosis. **2003**, *529*, 87–94. [https://doi.org/10.1016/S0027-5107\(03\)00106-4](https://doi.org/10.1016/S0027-5107(03)00106-4).
- (105) Buckley, B. J.; Tanswell, A. K.; Freeman, B. A. Liposome-Mediated Augmentation of Catalase in Alveolar Type II Cells Protects against H<sub>2</sub>O<sub>2</sub> Injury. *J. Appl. Physiol.* **1987**, *63* (1), 359–367. <https://doi.org/10.1152/jappl.1987.63.1.359>.
- (106) Lee, S.; Murthy, N. Targeted Delivery of Catalase and Superoxide Dismutase to Macrophages Using Folate. *Biochem. Biophys. Res. Commun.* **2007**, *360* (1), 275–279. <https://doi.org/10.1016/j.bbrc.2007.06.054>.
- (107) Yusa, T.; Crapo, J. D.; Freeman, B. A. Liposome-Mediated Augmentation of Brain SOD and Catalase Inhibits CNS O<sub>2</sub> Toxicity. *J. Appl. Physiol.* **1984**, *57* (6), 1674–1681. <https://doi.org/10.1152/jappl.1984.57.6.1674>.
- (108) Ozyilmaz, G.; Seyhan Tukel, S.; Alptekin, O. Kinetic Properties and Storage Stability of Catalase Immobilized on to Florisil. *Indian J. Biochem. Biophys.* **2007**, *44* (1), 38–43.
- (109) Brannan, T. S.; Maker, H. S.; Bernstein, M. Postmortem Stability of Enzymes Detoxifying Peroxide In Brain. *J. Neurochem.* **1982**, *39* (2), 589–591. <https://doi.org/10.1111/j.1471-4159.1982.tb03988.x>.
- (110) Konorev, E. A.; Kennedy, M. C.; Kalyanaraman, B. Cell-Permeable Superoxide Dismutase and Glutathione Peroxidase Mimetics Afford Superior Protection against Doxorubicin-Induced Cardiotoxicity: The Role of Reactive Oxygen and Nitrogen Intermediates. *Arch. Biochem. Biophys.* **1999**, *368* (2), 421–428. <https://doi.org/10.1006/abbi.1999.1337>.
- (111) Crocker, W. Catalase. In *Methods of Enzymatic Analysis (Second Printing, Revised)*; 1965; pp 885–894. <https://doi.org/10.1086/330448>.
- (112) Aebi, H. Catalase Invitro. *Methods Enzymol.* **1987**, *105* (1947), 121–126.
- (113) Sandstrom, P. A.; Buttke, T. M. Sandstrom 1993 - Autocrine Production of

Extracellular Catalase Prevents Apoptosis of.Pdf. **1993**, *90* (May), 4708–4712.

- (114) Darfler, F. J.; Insel, P. A. Clonal Growth of Lymphoid Cells in Serum-free Media Requires Elimination of H<sub>2</sub>O<sub>2</sub> Toxicity. *J. Cell. Physiol.* **1983**, *115* (1), 31–36. <https://doi.org/10.1002/jcp.1041150106>.
- (115) Mahan, L. C.; Insel, P. A. Use of Superoxide Dismutase and Catalase to Protect Catecholamines from Oxidation in Tissue Culture Studies. *Anal. Biochem.* **1984**, *136* (1), 208–216. [https://doi.org/10.1016/0003-2697\(84\)90327-0](https://doi.org/10.1016/0003-2697(84)90327-0).
- (116) Brubacher, J. L.; Bols, N. C. Chemically De-Acetylated 2', 7'-Dichlorodihydrofluorescein Diacetate As a Probe of Respiratory Burst Activity in Mononuclear Phagocytes. *J. Immunol. Methods* **2001**, *251*, 81–91.
- (117) Ohashi, T.; Mizutani, A.; Murakami, A.; Kojo, S.; Ishii, T.; Taketani, S. Rapid Oxidation of Dichlorodihydrofluorescein with Heme and Hemoproteins: Formation of the Fluorescein Is Independent of the Generation of Reactive Oxygen Species. *FEBS Lett.* **2002**, *511* (1–3), 21–27. [https://doi.org/10.1016/S0014-5793\(01\)03262-8](https://doi.org/10.1016/S0014-5793(01)03262-8).
- (118) Ding, Q.; Jin, T.; Wang, Z.; Chen, Y. Catalase Potentiates Retinoic Acid-Induced THP-1 Monocyte Differentiation into Macrophage through Inhibition of Peroxisome Proliferator-Activated Receptor  $\gamma$ . *J. Leukoc. Biol.* **2007**, *81* (6), 1568–1576. <https://doi.org/10.1189/jlb.1106672>.
- (119) Yamamoto, T.; Sakaguchi, N.; Hachiya, M.; Nakayama, F.; Yamakawa, M.; Akashi, M. Role of Catalase in Monocytic Differentiation of U937 Cells by TPA: Hydrogen Peroxide as a Second Messenger. *Leukemia* **2009**, *23* (4), 761–769. <https://doi.org/10.1038/leu.2008.353>.
- (120) Muscat, S.; Pelka, J.; Hegele, J.; Weigle, B.; Münch, G.; Pischetsrieder, M. Coffee and Maillard Products Activate NF- $\kappa$ B in Macrophages via H<sub>2</sub>O<sub>2</sub> Production. *Mol. Nutr. Food Res.* **2007**, *51* (5), 525–535. <https://doi.org/10.1002/mnfr.200600254>.
- (121) Nohl, H.; Kozlov, A. V.; Gille, L.; Staniek, K. Cell Respiration and Formation of Reactive Oxygen Species: Facts and Artefacts. *Biochem. Soc. Trans.* **2008**, *31* (6), 1308–1311. <https://doi.org/10.1042/bst0311308>.
- (122) Bolton, J. L.; Trush, M. A.; Penning, T. M.; Dryhurst, G.; Monks, T. J. Role of Quinones in Toxicology. *Chem. Res. Toxicol.* **2000**, *13* (3), 135–160. <https://doi.org/10.1021/tx9902082>.
- (123) Day., B. J. Catalase and Glutathione Peroxidase Mimics Brian. *Biochem. Pharmacol.* **2009**, *77* (3), 285–296. <https://doi.org/10.1038/mp.2011.182>.
- (124) Radi, R.; Cassina, A.; Hodara, R.; Quijano, C.; Castro, L. Peroxynitrite Reactions and Formation in Mitochondria. *Free Radic. Biol. Med.* **2002**, *33* (11), 1451–1464. [https://doi.org/10.1016/S0891-5849\(02\)01111-5](https://doi.org/10.1016/S0891-5849(02)01111-5).

- (125) Radi, R. Peroxynitrite, a Stealthy Biological Oxidant. *J. Biol. Chem.* **2013**, 288 (37), 26464–26472. <https://doi.org/10.1074/jbc.R113.472936>.
- (126) Wardman, P. Fluorescent and Luminescent Probes for Measurement of Oxidative and Nitrosative Species in Cells and Tissues: Progress, Pitfalls, and Prospects. *Free Radic. Biol. Med.* **2007**, 43 (7), 995–1022. <https://doi.org/10.1016/j.freeradbiomed.2007.06.026>.
- (127) Huan, Z.; Bannenberg, G. L.; Moldeus, P.; Shertzerl, H. G. Oxidation Pathways for the Intracellular 2',7'-Dichlorofluorescein. *Arch. Toxicol. Toxicol* **1994**, 582–587.
- (128) Tikku, M. L.; Liesch, J. B.; Robertson, F. M. Production of Hydrogen Peroxide by Rabbit Articular Chondrocytes. Enhancement by Cytokines. *J. Immunol.* **1990**, 145, 690–696.
- (129) Schonbaum, G. R.; Chance, B. Catalase. In *The Enzymes*; 1976; Vol. 13, pp 363–408.
- (130) Gomes, A.; Fernandes, E.; Lima, J. L. F. C. Use of Fluorescence Probes for Detection of Reactive Nitrogen Species: A Review. *J. Fluoresc.* **2006**, 16 (1), 119–139. <https://doi.org/10.1007/s10895-005-0030-3>.
- (131) Carreras, M. C.; Pargament, G. A.; Catz, S. D.; Poderoso, J. J.; Boveris, A. Kinetics of Nitric Oxide and Hydrogen Peroxide Production and Formation of Peroxynitrite during the Respiratory Burst of Human Neutrophils. *FEBS Lett.* **1994**, 341 (1), 65–68. [https://doi.org/10.1016/0014-5793\(94\)80241-6](https://doi.org/10.1016/0014-5793(94)80241-6).
- (132) Montiel-Dávalos, A.; Ibarra-Sánchez, M. de J.; Ventura-Gallegos, J. L.; Alfaro-Moreno, E.; López-Marure, R. Oxidative Stress and Apoptosis Are Induced in Human Endothelial Cells Exposed to Urban Particulate Matter. *Toxicol. Vitr.* **2010**, 24 (1), 135–141. <https://doi.org/10.1016/j.tiv.2009.08.004>.
- (133) Su, R.; Jin, X.; Zhang, W.; Li, Z.; Liu, X.; Ren, J. Particulate Matter Exposure Induces the Autophagy of Macrophages via Oxidative Stress-Mediated PI3K/AKT/MTOR Pathway. *Chemosphere* **2017**, 167, 444–453. <https://doi.org/10.1016/j.chemosphere.2016.10.024>.
- (134) Garçon, G.; Dagher, Z.; Zerimech, F.; Ledoux, F.; Courcot, D.; Aboukais, A.; Puskarić, E.; Shirali, P. Dunkerque City Air Pollution Particulate Matter-Induced Cytotoxicity, Oxidative Stress and Inflammation in Human Epithelial Lung Cells (L132) in Culture. *Toxicol. Vitr.* **2006**, 20 (4), 519–528. <https://doi.org/10.1016/j.tiv.2005.09.012>.
- (135) Kanupriya; Prasad, D.; Ram, M. S.; Kumar, R.; Sawhney, R. C.; Sharma, S. K.; Ilavazhagan, G.; Kumar, D.; Banerjee, P. K. Cytoprotective and Antioxidant Activity of *Rhodiola Imbricata* against Tert-Butyl Hydroperoxide Induced Oxidative Injury in U-937 Human Macrophages. *Mol. Cell. Biochem.* **2005**, 275 (1–2), 1–6. <https://doi.org/10.1007/s11010-005-7637-1>.

- (136) Zhou, J.; Bruns, E. A.; Zotter, P.; Stefenelli, G.; Prévôt, A. S. H.; Baltensperger, U.; El-Haddad, I.; Dommen, J. Development, Characterization and First Deployment of an Improved Online Reactive Oxygen Species Analyzer. *Atmos. Meas. Tech.* **2018**, *11* (1), 65–80. <https://doi.org/10.5194/amt-11-65-2018>.
- (137) Lardinois, O. M.; Mestdagh, M. M.; Rouxhet, P. G. Reversible Inhibition and Irreversible Inactivation of Catalase in Presence of Hydrogen Peroxide. *Biochim. Biophysica Acta* **1996**, *1295*, 222–238.
- (138) Arellanes, C.; Paulson, S. E.; Fine, P. M.; Sioutas, C. Exceeding of Henry's Law by Hydrogen Peroxide Associated with Urban Aerosols. *Environ. Sci. Technol.* **2006**, *40* (16), 4859–4866. <https://doi.org/10.1021/es0513786>.
- (139) Wang, Y.; Arellanes, C.; Curtis, D. B.; Paulson, S. E. Probing the Source of Hydrogen Associated with Coarse Mode Particles-Wang-2010.Pdf. *Environ. Sci. Technol.* **2010**, *44*, 4070–4075.
- (140) Wang, Y.; Arellanes, C.; Paulson, S. E. Hydrogen Peroxide Associated with Ambient Fine-Mode, Diesel, and Biodiesel Aerosol Particles in Southern California. *Aerosol Sci. Technol.* **2012**, *46* (4), 394–402. <https://doi.org/10.1080/02786826.2011.633582>.
- (141) Chung, M. Y.; Lazaro, R. A.; Lim, D.; Jackson, J.; Lyon, J.; Rendulic, D.; Hasson, A. S. Aerosol-Borne Quinones and Reactive Oxygen Species Generation by Particulate Matter Extracts. *Environ. Sci. Technol.* **2006**, *40* (16), 4880–4886. <https://doi.org/10.1021/es0515957>.
- (142) Wang, Y.; Kim, H.; Paulson, S. E. Hydrogen Peroxide Generation from  $\alpha$ - and  $\beta$ -Pinene and Toluene Secondary Organic Aerosols. *Atmos. Environ.* **2011**, *45* (18), 3149–3156. <https://doi.org/10.1016/j.atmosenv.2011.02.060>.
- (143) Lightfoot, P. D.; Cox, R. A.; Crowley, J. N.; Destriau, M.; Hayman, G. D.; Jenkin, M. E.; Moortgat, G. K.; Zabel, F. Organic Peroxy Radicals: Kinetics, Spectroscopy and Tropospheric Chemistry. *Atmos. Environ. Part A, Gen. Top.* **1992**, *26* (10), 1805–1961. [https://doi.org/10.1016/0960-1686\(92\)90423-I](https://doi.org/10.1016/0960-1686(92)90423-I).
- (144) Tong, H.; Arangio, A. M.; Lakey, P. S. J.; Berkemeier, T.; Liu, F.; Kampf, C. J.; Brune, W. H.; Poschl, U.; Shiraiwa, M. Hydroxyl Radicals from Secondary Organic Aerosol Decomposition in Water. *Atmos. Chem. Phys.* **2016**, *16* (3), 1761–1771. <https://doi.org/10.5194/acp-16-1761-2016>.
- (145) Guin, P. S.; Das, S.; Mandal, P. C. Electrochemical Reduction of Quinones in Different Media: A Review. *Int. J. Electrochem.* **2011**, *2011*, 1–22. <https://doi.org/10.4061/2011/816202>.
- (146) Charrier, J. G.; McFall, A. S.; Richards-Henderson, N. K.; Anastasio, C. Hydrogen Peroxide Formation in a Surrogate Lung Fluid by Transition Metals and Quinones Present in Particulate Matter. *Environ. Sci. Technol.* **2014**, *48* (12), 7010–7017.

<https://doi.org/10.1021/es501011w>.

- (147) Aschbacher, K.; O'Donovan, A.; Wolkowitz, O. M.; Dhabhar, F. S.; Su, Y.; Epel, E. Good Stress, Bad Stress and Oxidative Stress: Insights from Anticipatory Cortisol Reactivity. *Psychoneuroendocrinology* **2013**, *38* (9), 1698–1708. <https://doi.org/10.1016/j.psyneuen.2013.02.004>.
- (148) Liu, F.; Saavedra, M. G.; Champion, J. A.; Griendling, K. K.; Ng, N. L. Prominent Contribution of Hydrogen Peroxide to Intracellular Reactive Oxygen Species Generated upon Exposure to Naphthalene Secondary Organic Aerosols. *Environ. Sci. Technol. Lett.* **2020**. <https://doi.org/10.1021/acs.estlett.9b00773>.
- (149) Fisher, A. B. Redox Signaling Across Cell Membranes. *Antioxid. Redox Signal.* **2009**, *11* (6), 1349–1356. <https://doi.org/10.1089/ars.2008.2378>.
- (150) Rabolli, V.; Lison, D.; Huaux, F. The Complex Cascade of Cellular Events Governing Inflammasome Activation and IL-1 $\beta$  Processing in Response to Inhaled Particles. *Part. Fibre Toxicol.* **2016**, *13* (1), 1–17. <https://doi.org/10.1186/S12989-016-0150-8>.
- (151) Miller, E. W.; Dickinson, B. C.; Chang, C. J. Aquaporin-3 Mediates Hydrogen Peroxide Uptake to Regulate Downstream Intracellular Signaling. *Proc. Natl. Acad. Sci.* **2010**, *107* (36), 15681–15686. <https://doi.org/10.1073/pnas.1005776107>.
- (152) Meli, R.; Pirozzi, C.; Pelagalli, A. New Perspectives on the Potential Role of Aquaporins (AQPs) in the Physiology of Inflammation. *Front. Physiol.* **2018**, *9* (FEB), 1–11. <https://doi.org/10.3389/fphys.2018.00101>.
- (153) Tancharoen, S.; Matsuyama, T.; Abeyama, K.; Matsushita, K.; Kawahara, K.; Sangalungkarn, V.; Tokuda, M.; Hashiguchi, T.; Maruyama, I.; Izumi, Y. The Role of Water Channel Aquaporin 3 in the Mechanism of TNF- $\alpha$ -Mediated Proinflammatory Events: Implication in Periodontal Inflammation. *J. Cell. Physiol.* **2008**, *217* (2), 338–349. <https://doi.org/10.1002/jcp.21506>.
- (154) Rabolli, V.; Wallemme, L.; Lo Re, S.; Uwambayinema, F.; Palmari-Pallag, M.; Thomassen, L.; Tyteca, D.; Octave, J. N.; Marbaix, E.; Lison, D.; et al. Critical Role of Aquaporins in Interleukin 1 $\beta$  (IL-1 $\beta$ )-Induced Inflammation. *J. Biol. Chem.* **2014**, *289* (20), 13937–13947. <https://doi.org/10.1074/jbc.M113.534594>.
- (155) Xu, F.; Qiu, X.; Hu, X.; Shang, Y.; Pardo, M.; Fang, Y. Effects on IL-1 $\beta$  Signaling Activation Induced by Water and Organic. *Environ. Pollut.* **2018**, *237*, 592–600. <https://doi.org/10.1016/j.envpol.2018.02.086>.
- (156) Iles, K. E.; Dickinson, D. A.; Watanabe, N.; Iwamoto, T.; Forman, H. J. AP-1 ACTIVATION THROUGH ENDOGENOUS H<sub>2</sub>O<sub>2</sub> GENERATION BY ALVEOLAR MACROPHAGES KAREN. *Free Radic. Biol. Med.* **2002**, *32* (12), 1304–1313.

- (157) Kaul, N.; Forman, H. J. Activation of NF $\kappa$ B by The Respiratory Burst of Macrophages. *J. Natl. Cancer Inst.* **1996**, *21* (3), 401–405.
- (158) Brasier, A. R. The NF-KappaB Regulatory Network. *Cardiovasc. Toxicol.* **2006**, *6* (2), 111–130.
- (159) Tuet, W. Y.; Chen, Y.; Fok, S.; Champion, J. A.; Ng, N. L.; Sciences, A. Inflammatory Responses to Secondary Aerosols (SOA) Generated from Biogenic and Antropogenic Precursos. *Atmos. Chem. Phys. Discuss.* **2017**, No. March. <https://doi.org/10.5194/acp-2017-262>.